Three new species of *Axinulus* (Bivalvia: Thyasiridae) from the Japan and Kuril-Kamchatka trenches and abyssal zone of the northern Pacific Ocean (#83478)

First submission

Guidance from your Editor

Please submit by **10 Apr 2023** for the benefit of the authors (and your token reward) .

Structure and Criteria
Please read the 'Structure and Criteria' page for general guidance.

Custom checks
Make sure you include the custom checks shown below, in your review.

Author notes
Have you read the author notes on the guidance page?

Raw data check
Review the raw data.

Image check
Check that figures and images have not been inappropriately manipulated.

If this article is published your review will be made public. You can choose whether to sign your review. If uploading a PDF please remove any identifiable information (if you want to remain anonymous).

Files
Download and review all files from the materials page.

10 Figure file(s)
5 Table file(s)
2 Other file(s)

Custom checks

New species checks

- Have you checked our new species policies?
- Do you agree that it is a new species?
- Is it correctly described e.g. meets ICZN standard?

Structure and Criteria

Structure your review

The review form is divided into 5 sections. Please consider these when composing your review:

1. **BASIC REPORTING**
2. **EXPERIMENTAL DESIGN**
3. **VALIDITY OF THE FINDINGS**
4. General comments
5. Confidential notes to the editor

You can also annotate this PDF and upload it as part of your review

When ready submit online.

Editorial Criteria

Use these criteria points to structure your review. The full detailed editorial criteria is on your guidance page.

BASIC REPORTING

- Clear, unambiguous, professional English language used throughout.
- Intro & background to show context. Literature well referenced & relevant.
- Structure conforms to PeerJ standards, discipline norm, or improved for clarity.
- Figures are relevant, high quality, well labelled & described.
- Raw data supplied (see PeerJ policy).

EXPERIMENTAL DESIGN

- Original primary research within Scope of the journal.
- Research question well defined, relevant & meaningful. It is stated how the research fills an identified knowledge gap.
- Rigorous investigation performed to a high technical & ethical standard.
- Methods described with sufficient detail & information to replicate.

VALIDITY OF THE FINDINGS

- Impact and novelty not assessed. *Meaningful* replication encouraged where rationale & benefit to literature is clearly stated.
- All underlying data have been provided; they are robust, statistically sound, & controlled.
- Conclusions are well stated, linked to original research question & limited to supporting results.

Standout reviewing tips

The best reviewers use these techniques

Tip	*Example*
Support criticisms with evidence from the text or from other sources	*Smith et al (J of Methodology, 2005, V3, pp 123) have shown that the analysis you use in Lines 241-250 is not the most appropriate for this situation. Please explain why you used this method.*
Give specific suggestions on how to improve the manuscript	*Your introduction needs more detail. I suggest that you improve the description at lines 57- 86 to provide more justification for your study (specifically, you should expand upon the knowledge gap being filled).*
Comment on language and grammar issues	*The English language should be improved to ensure that an international audience can clearly understand your text. Some examples where the language could be improved include lines 23, 77, 121, 128 – the current phrasing makes comprehension difficult. I suggest you have a colleague who is proficient in English and familiar with the subject matter review your manuscript, or contact a professional editing service.*
Organize by importance of the issues, and number your points	*1. Your most important issue* *2. The next most important item* *3. …* *4. The least important points*
Please provide constructive criticism, and avoid personal opinions	*I thank you for providing the raw data, however your supplemental files need more descriptive metadata identifiers to be useful to future readers. Although your results are compelling, the data analysis should be improved in the following ways: AA, BB, CC*
Comment on strengths (as well as weaknesses) of the manuscript	*I commend the authors for their extensive data set, compiled over many years of detailed fieldwork. In addition, the manuscript is clearly written in professional, unambiguous language. If there is a weakness, it is in the statistical analysis (as I have noted above) which should be improved upon before Acceptance.*

Three new species of *Axinulus* (Bivalvia: Thyasiridae) from the Japan and Kuril-Kamchatka trenches and abyssal zone of the northern Pacific Ocean

Gennady M. Kamenev Corresp. 1

1 A.V. Zhirmunsky National Scientific Center of Marine Biology, Far Eastern Branch, Russian Academy of Sciences, Vladivostok, Russia

Corresponding Author: Gennady M. Kamenev
Email address: gennady.kamenev@mail.ru

The Thyasiridae is one of the species-richest families of bivalves in the deep-sea areas of the northern Pacific Ocean. Many thyasirid species form abundant populations in these regions and play an important role in the functioning of deep-sea benthic communities. However, most of these deep-sea thyasirid species have not been identified and many of them are new to science. Based on the material of bivalves collected by 8 deep-sea expeditions in the northern Pacific Ocean during the period from 1954 to 2016, three new species of the genus *Axinulus* (*Axinulus krylovae* sp. nov., *A. alatus* sp. nov., and *A. cristatus* sp. nov.) are described from the Kuril-Kamchatka and Japan trenches, the Bering Sea, and other deep-water regions of the northern Pacific Ocean (3,200–9,583 m depth). The new species are distinguished due to a unique and complex sculpture of the prodisoconch, including tubercles and numerous thin folds of varying length and shape, as well as due to a thickening of the shell in the adductor scar areas, thus rendering the scars raised above the inner surface of the shell. Comparisons with all species of the genus *Axinulus* are provided.

Three new species of *Axinulus* (Bivalvia: Thyasiridae) from the Japan and Kuril-Kamchatka trenches and abyssal zone of the northern Pacific Ocean

Gennady M. Kamenev

A.V. Zhirmunsky National Scientific Center of Marine Biology, Far Eastern Branch, Russian Academy of Sciences, Palchevskogo Str, 17, Vladivostok 690041, Russia

Corresponding Author:

Gennady M. Kamenev

Email address: gennady.kamenev@mail.ru

ABSTRACT

The Thyasiridae is one of the species-richest families of bivalves in the deep-sea areas of the northern Pacific Ocean. Many thyasirid species form abundant populations in these regions and play an important role in the functioning of deep-sea benthic communities. However, most of these deep-sea thyasirid species have not been identified and many of them are new to science. Based on the material of bivalves collected by 8 deep-sea expeditions in the northern Pacific Ocean during the period from 1954 to 2016, three new species of the genus *Axinulus* (*Axinulus krylovae* sp. nov., *A. alatus* sp. nov., and *A. cristatus* sp. nov.) are described from the Kuril-Kamchatka and Japan trenches, the Bering Sea, and other deep-water regions of the northern Pacific Ocean (3,200–9,583 m depth). The new species are distinguished due to a unique and complex sculpture of the prodisoconch, including tubercles and numerous thin folds of varying length and shape, as well as due to a thickening of the shell in the adductor scar areas, thus rendering the scars raised above the inner surface of the shell. Comparisons with all species of the genus *Axinulus* are provided.

INTRODUCTION

In recent years, international expeditions organized by the Russian Federation and Germany have sampled the deep-sea benthic fauna in an extensive region of the northwestern Pacific Ocean with depths of more than 3,000 m. The studies were focused on the composition and distribution of the benthic fauna in the deep-sea basins of the Seas of Japan and Okhotsk, the Kuril-Kamchatka Trench, and at the abyssal plain of the Pacific Ocean adjacent to the Kuril-

Kamchatka Trench (*Malyutina & Brandt, 2013; Brandt & Malyutina, 2015; Malyutina et al., 2018; Brandt et al., 2019*). Benthic macrofauna rich in species number and abundance was found in these deep-sea ecosystems, with bivalves being one of the dominant groups of animals (*Brandt et al., 2013, 2015, 2018, 2020; Kamenev, 2013, 2014, 2015, 2018a, b, c, 2019; Kamenev et al., 2022*). Among the bivalve fauna of all the studied deep-sea areas of the northwestern Pacific Ocean, the Thyasiridae was the species-richest family and many thyasirids were the dominant species in terms of abundance in the benthic macrofaunal communities (*Kamenev, 2013, 2015, 2018a, 2019; Kamenev et al., 2022*). At least 14 thyasirid species were found at depths greater than 3,000 m in the abyssal and hadal zones of the northwestern Pacific Ocean. They have not been identified to the species level and are most likely new to science. Moreover, previous studies of the northwestern Pacific deep-sea fauna revealed many species of thyasirids in various oceanic trenches (*Belyaev & Mironov, 1977; Belyaev, 1989; Okutani, Fujikura & Kojima, 1999; Allen, 2015*), most of them remain so far unidentified to the species level (*Belyaev, 1989*). Thus, despite the great importance of thyasirids in the functioning of the deep-sea ecosystems of the northwestern Pacific Ocean, the abyssal and hadal thyasirid fauna in the region is almost not studied, except three species (*Axinulus hadalis* (Okutani, Fujikura & Kojima, 1999), *Axinulus philippinensis* Allen, 2015, and *Thyasira kaireiae* (Okutani, Fujikura & Kojima, 1999)), which were found in the Japanese and Philippine trenches (*Okutani, Fujikura & Kojima, 1999; Allen, 2015*).

Several years ago, the author of this paper started a study of unidentified deep-sea species of the Thyasiridae found in the northwestern Pacific Ocean. As a result of this work, 6 new species have been described from the abyssal and hadal zones of the Sea of Okhotsk and the Bering Sea, the Kuril-Kamchatka and Japan trenches, as well as the oceanic plain adjacent to

these trenches (*Kamenev, 2020, 2023*). The present paper is a continuation the study of northwestern Pacific deep-sea thyasirids and presents a description of three new species of the genus *Axinulus* that were found in the Japan and Kuril-Kamchatka trenches, as well as in the abyssal zone of other deep-sea regions of the northern Pacific Ocean.

MATERIAL AND METHODS

Material studied

The material examined in this study was collected from 1954 to 1990 by expeditions of the P.P. Shirshov Institute of Oceanology, Russian Academy of Sciences, Moscow (IO RAS) in the hadal zone of the Kuril-Kamchatka Trench and from the Pacific abyssal plain adjacent to the Kuril-Kamchatka Trench (RV *Vityaz*, cruise no. 19, August 17 – October 29, 1954; RV *Vityaz*, cruise no. 39, July 7 – September 13, 1966), in the hadal zone of the Japan Trench (RV *Vityaz*, cruise no. 59, May 26 – July 5, 1976), in the Gulf of Alaska (RV *Vityaz*, cruise no. 45, April 23 – July 10, 1969), and from the bottom of the Commander Basin (Bering Sea) (RV *Akademik Mstislav Keldysh*, cruise no. 22, July 25 – October 27, 1990), as well as by the German-Russian deep-sea expeditions KuramBio (RV *Sonne*, cruise no. 223, July 21 – September 7, 2012) and KuramBio II (RV *Sonne*, cruise no. 250, August 16 – September 29, 2016) from the Pacific abyssal plain adjacent to the Kuril-Kamchatka Trench and in the hadal zone of the Kuril-Kamchatka Trench; and by the Russian-German deep-sea expedition SokhoBio (RV *Akademik M.A. Lavrentyev*, cruise no. 71, July 6 – August 6, 2015) in the abyssal zone of the Pacific slope of the Kuril Islands. The new species of Thyasiridae described here were found in 72 samples at depths of 3,200–9,583 m. Sampling during the IO RAS expeditions was carried out using an Okean grab (sampling area: 0.25 m^2), and Sigsbee and Galathea trawls (*Monin, 1983*). During

the KuramBio, KuramBio II, and SokhoBio expeditions a large box corer (sampling area: 0.25 m^2), epibenthic sledge, and Agassiz trawl were used (*Brandt & Malyutina, 2015; Malyutina et al., 2018; Brandt et al., 2020*). All samples collected by the IO RAS were fixed in 4% buffered formaldehyde, later transferred to 70% ethanol, and stored in the IO RAS Ocean Benthic Fauna collection (OBF). Samples collected by the KuramBio, KuramBio II, and SokhoBio expeditions were fixed in pre-cooled 96% ethanol and 4% buffered formaldehyde, transferred to 70% ethanol, and stored in the Museum (MIMB) of A.V. Zhirmunsky National Scientific Center of Marine Biology, Far Eastern Branch, Russian Academy of Sciences (NSCMB FEB RAS), Vladivostok (Russia). The type and other material of the new species described here was deposited in the collection of the MIMB, IO RAS OBF, and Senckenberg Museum Frankfurt, Germany (SMF).

Additional material was also examined for the comparison purposes: *Axinulus careyi* Bernard, 1979 (holotype, LACM 1990 (Natural History Museum of Los Angeles County, Los Angeles, USA)); paratype, SBNHM 55440 (Santa Barbara of the Natural History Museum, Santa Barbara)); *Axinulus kelliaeformis* Okutani, 1962 (holotype, NSMT Mo 69697 (National Museum of Nature and Science, Tsukuba, Japan)); *Axinulus thackergeigeri* Valentich-Scott & Coan, 2012 in Coan & Valentich-Scott, 2012 (holotype, SBNHM 149742; paratype, SBNHM 149743); *Axinulus obliquus* Okutani, 1968 (holotype, NSMT Mo 69719, and photos of paratype and additional specimens, NSMT Mo 69720 (photos by Dr. H. Saito)); *Clausina croulinensis* Jeffreys, 1847 (neotype, USNM 62048 (National Museum of Natural History), photos from USNM Web site); *Cryptodon (Axinulus) brevis* Verrill & Bush, 1898 (holotype, USNM 159873, photos from USNM Web site); *Cryptodon* (*Axinulus) simplex* Verrill & Bush, 1898 (holotype, USNM 159888, photos from USNM Web site); *Cryptodon equalis* Verrill & Bush, 1898

(holotype, USNM 74302, photos from USNM Web site); *Maorithyas hadalis* Okutani, Fujikura & Kojima, 1999 (paratype, NSMT Paratype C Mo 71432-c). Information and photos from USNM Web site provided with the permission of the National Museum of Natural History, Smithsonian Institution, 10th and Constitution Ave. N.W., Washington, DC 20560-0193 (http://www.nmnh.si.edu/).

Methods

Shell measurements were made using an ocular micrometer with an accuracy of 0.1 mm. Shell length (L), height (H), anterior end length (A), and shell width (W) were measured by using an ocular micrometer (Fig. 1). The ratios H/L, A/L, and W/L were determined.

For scanning electron microscopy, shells were cleaned of traces of soft tissues and periostracum in 50% diluted commercial bleach, washed in distilled water, and dried. They were then mounted to aluminium stubs using an adhesive tape and coated with chromium for examination with a SIGMA 300VP (Carl Zeiss, Cambridge, UK).

Gross anatomy was observed on preserved live-taken specimens. For anatomical studies, specimens of all species were dissected in 70% ethanol.

Microscopic observations of shells and bodies were performed in a Zeiss Discovery 8 stereomicroscope at the Far Eastern Center of Electron Microscopy of the NSCMB FEB RAS. The terminology of the shell morphology and body anatomy of the family Thyasiridae follows *Payne & Allen (1991)* and *Oliver & Killeen (2002)*.

Nomenclatural acts

The electronic version of this article in Portable Document Format (PDF) will represent a published work according to the International Commission on Zoological Nomenclature (ICZN), and hence the new names contained in the electronic version are effectively published under that Code from the electronic edition alone. This published work and the nomenclatural acts it contains have been registered in ZooBank, the online registration system for the ICZN. The ZooBank LSIDs (Life Science Identifiers) can be resolved and the associated information viewed through any standard web browser by appending the LSID to the prefix http://zoobank.org/. The LSID for this publication is: urn:lsid:zoobank.org:pub:0AE8C4E1-0F13-478E-81E9-287980139049. The online version of this work is archived and available from the following digital repositories: PeerJ, PubMed Central SCIE and CLOCKSS.

RESULTS

Systematics

Class Bivalvia

Order Lucinoida Gray, 1854

Superfamily Thyasiroidea Dall, 1900 (1895)

Family Thyasiridae Dall, 1900 (1895)

Genus *Axinulus* Verrill & Bush, 1898

Type species (by original designation): *Cryptodon (Axinulus) brevis* Verrill & Bush, 1898

Diagnosis: Shell small (<10 mm), equilateral or subequilateral, ovate to ovate-rhomboidal, slightly higher than long; margins entire, without any posterior sinus, but sometimes with weak

angulation of posterior margin; posterior sulcus absent or weak. Lunule variably expressed, indistinct to deep; escutcheon and auricle sometimes present. Hinge plate edentulous, sometimes with a small swelling. Ligament sunken, sometimes visible externally. Ctenidium of a single demibranch, foot vermiform, lateral body pouches without or with distinct lobes.

Remarks: Despite that the WoRMS (*WoRMS Editorial Board*, 2023) currently lists 13 species of the genus *Axinulus*, some authors (*Zelaya, 2010; Allen, 2015; Oliver, 2015; Kamenev, 2020*) recognize only 8 species as belonging to the genus (*Axinulus alleni* (Carrozza, 1981), *Axinulus brevis* (Verrill & Bush, 1898), *Axinulus croulinensis* (Jeffreys, 1847), *Axinulus antarcticus* Zelaya, 2010, *A. philippinensis*, *Axinulus subequatorius* (Payne & Allen, 1991), *Axinulus oliveri* Kamenev, 2020, and *Axinulus roseus* Kamenev, 2020). Therefore, the new species described herein were compared only with the above species. Assignment the other 5 species to the genus *Axinulus* is doubtful (*Oliver, 2015; Kamenev, 2020*).

***Axinulus krylovae* sp. nov.**

(Figs. 2–5, Tables 1, 2)

Axinulus sp.: *Kamenev, 2015*, p. 191.

"*Genaxinus*" sp. 1: *Kamenev, 2019*, p. 6, 7.

urn:lsid:zoobank.org:act:F3D588B6-84FD-44A7-99BF-7FB53AC893F3

Type material and locality: Holotype (IORAS XXXXX), Japan Trench, Pacific Ocean (36°44'N, 143°19'E), 7,540 m, Galathea trawl, Coll. F.A. Pasternak, 23-VI-1976 (RV *Vityaz*, cruise no. 59, stn. 7503); paratypes (4) (IORAS XXXXX) and paratype (MIMB XXXXX) from holotype locality; paratype (MIMB XXXXX) and paratype (SMF (Senckenberg Museum Frankfurt) XXXXX), Kuril-Kamchatka Trench, Pacific Ocean (45°56.821'N, 152°51.185'E –

45°56.834'N, 152°50.943'E), 6,168-6,164 m, epibenthic sledge, Coll. A. Brandt, 27-VIII-2016 (RV *Sonne*, cruise no. 223, stn. 30).

Other material examined: 438 live specimens (Table 1).

Diagnosis: Shell medium in size (to 5.2 mm in length), elongated ovate to rhomboidal, with two radiating, whitish, elongated triangular rays extending from beaks to anteroventral and posteroventral margins. Sculpture of closely spaced commarginal riblets forming weak undulations and conspicuous, closely spaced, radial ribs and rays as slightly convex overlap areas of varying width over commarginal riblets. Posterior folds and sulcus absent. Escutcheon and auricle absent. Lunule as a crest, raised, wide, weakly defined. Ligament sunken, only slightly visible externally, long. Prodissoconch small (length 131-158 µm), irregularly convex, with distinct tubercle in anterior part; initial part sculptured densely spaced, chaotically located, short, curved plicae and numerous, radial, thin folds. Adductor muscle scars distinct, outline elongated triangular, raised above inner shell surface because of thickening of shell. Lateral body pouches large, simple, without numerous distinct lobes.

Description. Shell medium in size (to 5.2 mm in length and 5.7 mm in height), strongly inflated (W/L=0.671±0.028), slightly higher than long (H/L=1.083±0.039); elongated ovate to rhomboidal, equivalve, subequilateral, white, thick, with two curved, radial, whitish, elongated triangular, opaque rays extending from beaks to anteroventral and posteroventral margins, respectively, formed by internal thickening shell; patches of silty deposit adhering to anteriodorsal and posterior shell margins (Fig. 2, Table 2). Periostracum thin, colorless, translucent, adherent. Dissoconch sculptured with thin, closely spaced, commarginal riblets forming weak, narrow, irregular, undulations and conspicuous, closely spaced, radial ribs and

rays ~~as~~ overlap areas of varying width over commarginal riblets. Beaks small, raised, prosogyrate, curved slightly inwards, slightly anterior to midline (A/L=0.415±0.032) (Fig. 3, Table 2). Anterodorsal shell margin convex, steeply sloping from beaks, forming a rounded angle at transition to anterior margin. Anterior margin curved, smoothly transitioning to ventral margin. Ventral margin strongly curved, sometimes slightly angulate. Posterodorsal margin slightly convex, steeply sloping from beaks, smoothly transitioning to posterior margin. Posterior margin slightly curved or straight, smoothly transitioning to ventral margin. Posterior folds and sulcus absent but posterior shell area a little flattened. Escutcheon and auricle absent. Lunule as a crest, raised, long, wide, weakly defined, demarcated by weak, long, rounded ridges along entire anterodorsal shell margin (Figs. 3D, C). Ligament opisthodetic, sunken, slightly visible externally as a narrow strip between valves, thick, almost straight, long, about half the length of posterodorsal shell margin, lying in deep, slightly curved, wide groove at surface of hinge plate (Fig. 4). Prodissoconch small (length 131-158 µm), ovate in outline, slightly drawn out anteriorly, irregularly convex, flattened anteriorly, with a distinct tubercle and shallow depression in initial part (Figs. 3M-T). Tubercle and depression of prodissoconch sculptured with numerous, densely spaced, short and chaotically ~~located~~ folds, forming a rounded area; numerous short, thin, radial folds of about same length radiating from this area; remaining surface of prodissoconch smooth or slightly bumpy (Fig. 3N). Hinge plate thickened, with a small, distinct tubercle under beak in each valve and long, deep ligamental groove (Fig. 4). Adductor muscle scars distinct, long, elongated triangular in outline, extending into umbonal cavity, bearing thin, indistinct, radial striation; shell strongly thickened in scar area, thus rendering muscle scars raised above inner shell surface. Posterior adductor scar narrow, straight; anterior adductor scar curved, approximately twice as wide as posterior (Fig. 4).

Gross anatomy: Mantle thin; margins thickened and unfused except limited interconnection at the posterior ventral margin with a small exhalant aperture below the posterior adductor muscle (Fig. 5A). Anterior adductor muscle elongated, 2 times longer than posterior adductor, slightly curved parallel to anterodorsal shell margin, dorsal part narrower than ventral part. Posterior adductor muscle small, oval. Ctenidium thin, narrow, consisting of a single inner demibranch with fully reflected filaments (up to 50 filaments in large specimens more than 4.7 mm in length). Demibranch not covering lateral body pouches and consisting of both ascending and descending lamellae; ascending lamellae slightly shorter than descending lamellae. Labial palps small (to 150 μm), triangular, located at proximal end of longer (more than 1 mm) oral grooves extending to antero-ventral corner of gill (Figs 5B-F). Lateral pouches large (Figs. 5B, C, J, M, N), dorsoventrally elongated, oval in outline, with undulated margins and a few small, slightly projecting lobes along different margins; each pouch connecting to body by a wide neck (Figs. 5D-F). Kidneys large, elongated, occupying a posterodorsal position between posterior adductor muscle and heart, containing numerous, bright orange, large (to 80 μm in diameter), different-size granules (Figs. 5D, J, H). Gonad occupying inner side of lateral pouches. Sexes are separate. Eggs oval or polygonal (up to 120-130 μm in length after fixation) (Fig. 5L). Alimentary system with short esophagus leading to a relatively large, elongate stomach; combined style sac and strongly curved midgut forming a deep and narrow loop between neck of lateral pouches and kidney; hind gut forming an anterior, deep, and wide loop dorsal to style sac, running posteriorly dorsal to kidney and posterior adductor muscle, opening at ventral side of posterior adductor muscle (Figs. 5I, P). Foot long, vermiform, depending upon its state of contraction, may either form coil within mantle cavity or form a relatively short, curved steam

with bulbous tip; surface of bulbous portion with densely spaced papillae (Figs. 5D, K, N). Heel absent. Anterior and posterior pedal retractors short, narrow (Figs. 5D, F).

Variability: The shell shape and proportions, the degree of slope of anterodorsal and posterodorsal shell margins and curving of all shell margins vary significantly among different sized specimens (Figs. 2-4, Table 2). Some specimens have a shell rather elongated dorsoventrally and ovate in outline. In some specimens, the shell is more rounded and angulate, the anterodorsal and posterodorsal margins are sloped more gently from beaks, the anterodorsal margin is more convex and the posterodorsal margin is almost straight, the ventral margin is more curved and slightly drawn out anteriorly. Moreover, in thicker-shelled specimens the hinge plate is wider and the inner thickenings of the shell in the adductor muscle scar areas are much thicker and more expressed compared with specimens with a thinner shell (Figs. 4I, M, R, T).

Distribution: This species was recorded on the oceanic slope of the Kuril Islands (45°01.202′N, 151°06.008′E–47°14.32′N, 154°42.26′E) at a depth of 4,982–5,766 m, on the abyssal plain adjacent to the Kuril-Kamchatka Trench (39°43.43′N, 147°09.98′E–46°13.99′N, 155°33.10′E) at a depth of 4,860–5,497 m (bottom temperature (6–8 m above bottom) 1.5–1.6 °C, salinity 34.7‰, oxygen 7.71–7.72 ml. l^{-1}) (*Brandt et al. 2015*), in the Kuril-Kamchatka Trench (44°06.152′N, 151°25.705′E–45°56.821′N, 152°51.185′E) at a depth of 6,068–9,540 m, and in the Japan Trench (36°44′N, 143°19′E–38°38′N, 144°06′E) at a depth of 7,350–7,540 m.

Comparisons: *Axinulus krylovae* sp. nov. strongly differs from all species of the genus *Axinulus* in having expressed thickenings of the shell in the adductor muscle scar areas, which are visible on the outer surface of the anterior and posterior parts of the shell as wide radial rays extending from the beaks (Table 3). Due to the shell thickening, the muscle scars are raised to various

degrees above the inner shell surface, depending on the thickness of the shell itself. Also, *Axinulus krylovae* sp. nov. is clearly distinguished from all the other species by a unique sculpture of the prodissoconch (Table 3). Moreover, the new species well differs from almost all species of the genus *Axinulus* in having a conspicuous radial sculpture of the shell. Judging by photos of the type material and descriptions of species, *A. brevis*, *A. croulensis*, and *A. philippinensis* also have a radial sculpture on the shell surface, but it is less distinct and was described as fine radial lines or a peculiar radial texture (*Oliver & Killeen, 2002; Allen, 2015*). In contrast to most species of the genus, the new species has a larger shell. Only *A. oliveri* and *A. roseus* also have a large shell, but unlike *Axinulus krylovae* sp. nov., their shells lack the radial sculpture and inner thickenings in the adductor muscle scar areas and are characterized by a well- defined escutcheon (*Kamenev, 2020*). In addition, the above species have extensively lobed lateral pouches.

Derivation of name: The new species was named in honor of the well-known malacologist E.M. Krylova, who made a significant contribution to the study of the world fauna of the family Vesicomyiidae and the superfamily Cuspidarioidea and has always provided invaluable help in my research on the deep-sea bivalve fauna of the northern Pacific.

Remarks: *Axinulus krylovae* sp. nov. has more or less expressed inner thickenings of the shell, depending on the shell thickness, in the area of adductor muscle scars. As a result, the muscle scars are raised above the inner shell surface. The thickened shell area is, as a rule, more pronounced posteriorly than anteriorly. The presence of elevated adductor scars is a characteristic and main distinguishing feature of species of the genus *Genaxinus* Iredale, 1930 from other genera of the family Thyasiridae (*Hedley, 1907; Iredale, 1930; Oliver & Killeen, 2002; Oliver & Levin, 2006; Oliver, 2015*). Nevertheless, I think the new species should be

assigned to the genus *Axinulus* but not to *Genaxinus*. In species of *Genaxinus*, only muscle scars themselves are raised. The new species has the thickened anterior and posterior parts of shell, which are larger in area than the muscle scars proper, and these thickened areas bear muscle scars. The degree of inner shell thickening significantly varies, thus influencing the degree of elevation of muscle scars above the inner shell surface. Unlike the species described herein, in species of the genus *Genaxinus*, muscle scars bear prominent concentric growth marks that were formed during migration of the muscle during growth. In the *Genaxinus* species, the muscle scars are white color, project from the inner shell surface, and are well visible through the shell from outside (*Payne & Allen, 1991; Oliver & Killeen, 2002*).

The thickenings of the shell in muscle scar areas analogous to those of *Axinulus krylovae* sp. nov. are also characteristic of other species of the Thyasiridae (e.g., *A. croulinensis*, *A. alleni*, *Mendicula ultima* (Payne & Allen, 1991)) (*Payne & Allen, 1991; Oliver & Killeen, 2002*). In these species, inner shell thickening is also more expressed in the posterior area of the shell. Most probably, thorough studies of small thyasirids using scanning electron microscopy will reveal analogous inner shell thickenings in some other species as well.

The new species described here has a wide geographic and vertical distribution in the northwestern Pacific Ocean. It was found in large numbers in many samples from this vast region. This allowed a study of both the age and individual variability of its shell morphology. On the whole, the shell shape and proportions vary greatly, irrespective of the sampling area and depth. Specimens found in different areas and at different depths were of different size and had both the rounded and dorsoventrally elongated shell shape. A thorough examination of the shell morphology of specimens from various parts of the species range showed that they have the same main morphological characters (shell sculpture, hinge plate morphology, inner shell

thickenings in muscle scar areas, prodissoconch sculpture). I found no unique morphological and anatomical features characteristic of a group of specimens. Moreover, specimens with a transitional shape of the shell between elongated oval and almost rounded were found in samples. Therefore, I think that specimens with different shell shape belong to the same species. It should be noted that many species of the Thyasiridae, among them species of *Axinulus*, exhibit a large age and individual variability of the shell shape and proportions (*Payne & Allen, 1991; Oliver & Killeen, 2002; Allen, 2015; Kamenev, 2020*).

Axinulus krylovae sp. nov. was found in the Pacific Ocean in a wide depth range (about 5,000 m). An earlier study recorded 3 species of bivalves with a vertical distribution range of 4,000 to 7,000 m among the hadal fauna of the Kuril-Kamchatka Trench. In addition, a number of eurybathic species from various taxonomic groups have a vertical distribution range greater than 5,000–7,000 m (*Kamenev, 2019*). By all appearances, *A. krylovae* sp. nov. also belongs to the group of eurybathic species inhabiting a wide depth range in the abyssal and hadal zones of the Pacific Ocean.

***Axinulus alatus* sp. nov.**

(Figs. 6-9, Tables 4, 5)

Axinulus sp.: *Kamenev,* 2018, p. 234.

urn:lsid:zoobank.org:act:0BBDAC37-2258-4C8B-89E4-DECF7402C58E

Type material and locality: Holotype (MIMB XXXXX), slope of the Kuril Islands, Pacific Ocean (46°16.082'N, 152°02.060'E), 3,432 m, boxcorer, Coll. G.M. Kamenev, 27-VII-2015 (RV *Akademik M.A. Lavrentyev*, cruise no. 71, stn. 9-1); paratype (SMF XXXXX), from holotype locality; paratypes (5) (IORAS XXXXX) and paratype (MIMB XXXXX), Commander Basin,

328 Bering Sea (55°13.2'N, 167°29.07'E – 55°12'N, 167°26.7'E), 3,957–3,978 m, Sigsbee trawl, Coll.
329 S.V. Galkin, 31-VII-1990 (RV *Akademik Mstislav Keldysh*, cruise no. 22, stn. 2309).

330 **Other material examined:** 89 live specimens (Table 4).

331 **Diagnosis:** Shell small (to 2.9 mm in length), oval to ovate-polygonal, slightly drawn out
332 anterior, with two slightly curved, radiating, whitish, elongate-triangular, opaque rays extend
333 from beaks to anteroventral and posteroventral margins. Sculpture of closely spaced,
334 commarginal riblets. Micro-sculpture of densely spaced pits. Posterior folds and sulcus absent.
335 Escutcheon long, narrow, shallow. Auricle long, low. Lunule as a weak crest, slightly raised,
336 short, lanceolate. Ligament sunken, not visible externally, short. Prodissoconch medium in size
337 (length 161-174 μm); initial part with small area of densely spaced, short, curved folds and
338 wrinkles and two series of commarginal, long, thin folds extending as wings from this area.
339 Adductor muscle scars distinct, elongated triangular in outline; posterior scar raised above inner
340 shell surface due to thickening of shell. Lateral body pouches small, simple, without projecting
341 lobes.

342 **Description.** Shell small (to 2.9 mm in length and 3.1 mm in height), inflated
343 (W/L=0.618±0.024), higher than long (H/L=1.105±0.026), slightly drawn out anteriorly, median
344 area divided by a weak change in angulation; oval to ovate-polygonal, sometimes slightly
345 pyriform, subequilateral, white, thin, translucent, with two slightly curved, radiating, whitish,
346 elongate-triangular, opaque rays extending from beaks to anteroventral and posteroventral
347 margins, respectively, more marked in posterior shell area, formed by internal thickening of shell
348 associated with anterior and posterior adductor muscles; patches of silty deposit adhering to
349 anterior and posterior shell margins (Fig. 6, Table 5). Periostracum very thin, colorless,

translucent, adherent. Dissoconch sculptured with thin, closely spaced, commarginal riblets. Micro-sculpture of small, densely spaced pits. Beaks small, prosogyrate, curved slightly inwards, anterior to midline (A/L=0.369±0.033) (Fig. 7, Table 5). Anterodorsal shell margin long, convex, steeply sloping from beaks, forming a rounded angle at transition to anterior margin. Anterior shell margin curved, smoothly transitioning to ventral margin. Ventral margin strongly curved, slightly angulate. Posterodorsal shell margin long, convex, steeply sloping from beaks, forming a broadly rounded angle at transition to posterior margin. Posterior shell margin slightly curved, smoothly transitioning to ventral margin. Posterior folds absent but posterior shell area a little flattened. Escutcheon long, almost as long as entire length of posterodorsal shell margin, narrow, shallow, demarcated by low ridges. Auricle long, almost as long as entire length of escutcheon, weak, low, only slightly projecting (Figs. 7B, C, G). Lunule as a weak crest, slightly raised, short, about half length of anterodorsal shell margin, narrow, lanceolate, weakly defined by low and thin ribs (Fig. 7D). Ligament opisthodetic, sunken, not visible externally, short, about one third of entire length of the escutcheon, thick, almost straight, lying in deep, wide groove in hinge plate (Figs. 7L-N, P-R). Prodissoconch medium in size (length 161-174 μm), distinctly separated from dissoconch, ovate in outline. Initial part of prodissoconch with densely spaced, short, curved folds and wrinkles interspersed with pits, forming a rounded zone. This zone giving rise to 2 series of commarginal, long, thin, low folds (about 20 folds in each series), extending as wings in different directions; remaining surface of prodissoconch smooth (Fig. 8). Hinge plate thin, edentulous, with almost straight ligamental groove (Figs. 7L, P). Adductor muscle scars distinct, long, elongated triangular in outline, extending into umbonal cavity, bearing thin, radial striation. Posterior adductor scar narrow, straight, raised above inner shell surface due to

thickening of shell in this area. Anterior adductor scar wider than posterior one, curved, not raised above inner shell surface (Figs. 7K, M, O, Q).

Anatomy: Mantle thin; margins thickened, unfused except long posterior suture with two exhalant apertures below the posterior adductor (Fig. 9A). Anterior adductor muscle elongated, 2 times longer than posterior adductor, slightly curved, dorsal part narrower than ventral part. Posterior adductor muscle small, oval (Figs. 9B, C). Ctenidium thin, narrow, consisting of a single inner demibranch with fully reflected filaments (up to 30 filaments in largest specimen 2.9 mm in shell length). Demibranch not covering lateral body pouches and consisting of both ascending and descending lamellae; ascending lamellae slightly shorter than descending lamellae. Labial palps small, as extensions of the short (about 300 μm), oral grooves (Fig. 9B). Lateral body pouches small (Figs. 9C, F), dorsoventrally elongated, outline oval, with undulated margins, without projecting lobes; each pouch connecting to body by a wide neck (Fig. 9D). Kidneys large, dorsoventrally elongated along posterodorsal shell margin, without granules (Figs. 7C-G). Alimentary system with short oesoghagus leading to an elongate stomach; combined style sac and midgut strongly curved, forming a deep and narrow loop between neck of lateral pouches and kidney; hind gut forming an anterior, deep, and wide loop dorsal to style sac, running posteriorly dorsal to kidney and posterior adductor muscle, opening at ventral side of posterior adductor muscle (Figs. 7E, H). Foot long, vermiform, distally bulbous, with a muscular ring at the junction with the visceral mass. Bulbous portion of foot not divided into two distinct parts; surface with densely spaced papillae; heel absent. Anterior and posterior pedal retractors short, narrow (Figs. 7B, C, F).

Variability: The shell shape and proportions vary little among different-sized specimens (Figs. 6G-M, Table 5). The shell shape is oval to ovate. Some specimens have a more angular

and relatively shortened shell. In small specimens (less than 2 mm in shell length), the shell is more elongated dorsoventrally, with a more anteriorly drown-out ventral margin.

Distribution: This species was recorded on the oceanic slope of the Kuril Islands (46°16.082′N, 152°02.060′E–46°16.129′N, 152°03.324′E) at a depth of 3,377–3,436 m, at the bottom of Commander Basin (Bering Sea) (55°12.7′N, 167°26.7′E–55°36.1′N, 167°23.04′E) at a depth of 3,957–4,294 m, and off Kodiak Island (Gulf of Alaska, Pacific Ocean) (57°37.7′N, 148°34.5′W) at a depth of 3,200 m.

Comparisons: *Axinulus alatus* sp. nov. differs from all species of the genus *Axinulus* in having a unique sculpture of the prodissoconch (Table 3). In terms of the shape, proportions, and size of the shell, *A. alatus* sp. nov. is closest to *A. brevis*, *A. croulensis*, *A. antarcticus*, and *A. subequatorius*. However, unlike *A. brevis* and *A. croulensis*, the new species described here lacks radial sculpture of the shell and has a well-defined, long auricle, and a deep sunken ligament invisible externally. Apart from the differences in prodissoconch sculpture, *A. alatus* sp. nov. is distinguished from *A. antarcticus* by having a long lanceolate lunule and a deep sunken ligament invisible externally. *Axinulus alatus* sp. nov. differs from *A. subequatorius* in lacking projecting lobes of lateral body pouches and in having two posterior inhalant apertures but not one (*Payne & Allen, 1991*).

Derivation of name: The species epithet meaning “winged” indicates the similarity of two series of long, commarginal folds of the prodissoconch to the extended wings of a flying bird.

Remarks: *Axinulus alatus* sp. nov. has a wide range in the northern Pacific Ocean and was found off the Asian and American continents in the lower abyssal zone in the depth range of 3,000-5,000 m. The species was not found among extensive material of bivalves collected by the numerous deep-sea expeditions at depths greater than 5,000 m at the abyssal plain adjacent to the

Kuril-Kamchatka and Japan trenches (*Okutani, 1974, 2000; Okutani & Fujikara, 2002; Okutani & Kawamura, 2002; Kamenev, 2015, 2018a*), as well as in the hadal zone of the Aleutian, Kuril-Kamchatka, and Japan trenches (*Okutani, 1974, 2003; Okutani, Fujikura & Kojima, 1999; Fujikura et al., 1999, 2002; Okutani & Fujiwara, 2005; Kamenev, 2019, 2020, 2023*). In addition, this species was not recorded for the benthic fauna of the Kuril Basin (the Sea of Okhotsk) a little less than 3,300 m deep (*Kamenev,* 2018a), though it was found on the oceanic slope of the Kuril Islands opposite the deepest Bussol Strait connecting the Sea of Okhotsk and the Pacific Ocean. The deep-sea ecosystem of the Kuril Basin is characterized by low oxygen concentrations near the bottom, largely influencing the composition and quantitative distribution of benthic fauna (*Kamenev et al., 2022*). It is possible that oxygen deficiency exerts a negative influence, not allowing the species to live in the Kuril Basin. In the Commander Basin (Bering Sea), in contrast to the Kuril Basin, *A. alatus* sp. nov. forms high-density populations. Probably, *A. alatus* sp. nov. is a low abyssal species, preferring depths of 3,000–5,000 m.

***Axinulus cristatus* sp. nov.**

(Fig. 10)

urn:lsid:zoobank.org:act:BFDA7E99-6561-4597-B5BE-5037F42815B0

Type material and locality: Holotype (MIMB XXXXX), Kuril-Kamchatka Trench, Pacific Ocean (45°56.821'N, 152°51.185'E – 45°56.834'N, 152°50.943'E), 6,168–6,164 m, epibenthic sledge, Coll. A. Brandt, 27-VIII-2016 (RV *Sonne*, cruise no. 223, stn. 30).

Diagnosis: Shell medium in size (to 3.6 mm in length), pyriform. Sculpture of closely spaced, commarginal ribs and narrow, radial rays consisting of finest, short, concentric wrinkles. Posterior folds and sulcus absent. Escutcheon and auricle absent. Lunule as a weak crest, raised,

long, wide, weakly defined. Ligament sunken, long. Prodissoconch small (length 127 µm), with 24 thin, almost straight folds of different length, extending from high crest, located in mid-line of prodissoconch. Adductor muscle scars distinct, elongated triangular in outline, not raised above inner surface of shell. Inner shell surface with distinct, thin, radial striae.

Description. Shell medium in size (to 3.6 mm in length and 3.8 mm in height), pyriform, equivalve, subequilateral, white, thick, inflated, slightly higher than long (H/L=1.043) (Fig. 10). Periostracum thin, colorless, translucent, adherent. Dissoconch sculptured with thin, closely spaced, commarginal ribs and narrow, closely spaced, radial rays of varying width, formed by closely spaced, finest, short, concentric wrinkles; radial rays becoming widest and prominent along shell margins (Figs. 10B-D). Beaks small, raised, prosogyrate, anterior to midline (A/L=0.312). Anterodorsal shell margin convex, steeply sloping from beaks, smoothly transitioning to anterior margin. Anterior margin curved, smoothly transitioning to ventral margin. Ventral margin gently curved. Posterodorsal margin long, slightly convex, steeply sloping from beaks, descending to mid-point of shell, forming a rounded angle at transition to slightly curved posterior margin. Posterior folds and sulcus absent. Escutcheon and auricle absent. Lunule as a weak crest, raised, long, wide, weakly defined, demarcated by weak, long, rounded ridges along entire anterodorsal shell margin. Ligament opisthodetic, sunken, thick, evenly curved, long, about half the length of posterodorsal shell margin, lying in deep, curved groove at surface of hinge plate (Figs. 10E-G). Prodissoconch small (length 127 µm), distinct, oval in outline, convex, with 24 thin, almost straight folds of different length, sometimes bifurcated at end, extending from a long, high crest, located in mid-line of prodissoconch; remaining surface of prodissoconch smooth (Figs. 10J-M). Hinge plate thickened, with a distinct, flattened, spoon-shaped tubercle under beak in left valve and a long ligamental groove (Figs.

10G-I). Adductor muscle scars distinct, long, outline elongated triangular, extending into umbonal cavity, bearing thin, indistinct, radial striation, not raised above shell surface. Posterior adductor scar narrow, straight. Anterior adductor scar about two times wider than posterior and curved. Inner shell surface with distinct, thin, radial lines, corresponding to radial sculpture of external shell surface (Figs. 10E, F).

Distribution: This species is known only from the holotype locality in the Kuril-Kamchatka Trench at a depth of 6,168–6,164 m.

Comparisons: *Axinulus cristatus* sp. nov. is readily distinguished from all species of the genus *Axinulus* in having a radial sculpture in the form of rays consisting of closely spaced, short, finest, wrinkles and distinct radial lines on the inner shell surface, as well as by its unique sculpture of the prodissococh (Table 3). In addition, the new species differs from other species of the genus *Axinulus* in having a distinct spoon-shaped tubercle on the hinge plate in the left valve. However, the unusual shape of the tubercle on the hinge plate may be an individual abnormality of the examined specimen rather than being a specific character.

Derivation of name: The species name means “crested” and refers to a high crest on the surface of the prodissoconch.

Remarks: Unfortunately, only a single specimen of *A. cristatus* sp. nov. was found after examining all the material collected by many expeditions in the northwestern Pacific Ocean. Therefore, the gross anatomy of the body of this species is not studied, because the body has partially dissolved during preparation of the specimen for examination in a scanning microscope. In the specimen described here, the gill had only one demibranch; therefore, I assigned the species to the genus *Axinulus*. Since the shell of the species has a number of unique

morphological characters that readily separate it from the congeners, I described it as new to science, despite the minimal material at my disposal. Due to the difficulty of collecting bottom animals from great depths, many deep-sea species are often represented by a single specimen in the benthic fauna collections made by different deep-sea expeditions (*Kamenev, 2015, 2019*) and are thus described from merely 1-2 specimens (e.g., *Knudsen, 1970; Payne & Allen, 1991*).

Discussion

Until recently, the genus *Axinulus* was represented only by 6 species (*Zelaya, 2010; Allen, 2015; Oliver, 2015; Kamenev, 2020*). Of these, 5 species were found in the Atlantic Ocean (*Payne & Allen, 1991; Allen, 2008; Zelaya, 2010*), while in the Pacific Ocean only one species of the genus, *A. philippinensis*, was recorded and described from the bottom of the Philippine Trench (*Allen, 2015*). In recent years, a study of the extensive material of bivalves collected by many deep-sea expeditions mainly in the northwestern Pacific Ocean, another 5 species of the genus *Axinulus* were recorded for the Pacific Ocean (*Kamenev, 2020*). Thus, the number of species in the genus has increased almost twice, and at present the fauna of *Axinulus* in the Pacific Ocean has more species, compared to the Atlantic Ocean.

Out of all the species found in the Atlantic Ocean, only *A. subequatorius* was recorded exclusively in the abyssal zone at depths of more than 3,000 m. The other species have a wider vertical distribution range and were recorded in the subtidal and bathyal zones at depths less than 3,000 m. In contrast to Atlantic species, all Pacific species of the genus *Axinulus* were found exclusively at depths greater than 3,000 m. Moreover, almost all of them, except *A. alatus* sp. nov., were recorded in the hadal zone of different oceanic trenches at depths of more than 6,000 m (*Allen, 2015; Kamenev, 2020*). Thus, unlike the Atlantic Ocean, species of the genus *Axinulus* are typical members of the abyssal and hadal benthic fauna in the northern Pacific Ocean. In

addition, the species *A. roseus*, *A. krylovae* sp. nov., *A. philippinensis*, and *A. alatus* sp. nov. were found in large numbers in samples collected from the floor of the deepest basins of the Kuril-Kamchatka, Japan, and Philippine trenches, and the Bering Sea, respectively (*Allen, 2015; Kamenev, 2020; Kamenev et al., 2022*), where they probably play a substantial role in the functioning of benthic deep-sea ecosystems in these northwestern Pacific regions.

Presumably, species of the genus *Axinulus* were found in another 7 oceanic trenches, apart from the Kuril-Kamchatka, Japan, and Philippine trenches (*Belyaev, 1989*). Therefore, further study will most likely increase the species richness of the genus *Axinulus*.

Unlike many species of the genus *Thyasira*, many species of the genus *Axinulus* have a unique sculpture ~~of the~~ prodissoconch, which is one of the important diagnostic characters of thyasirids (*Zelaya, 2009, 2010; Kamenev, 2020, 2023*). The prodissoconch sculpture of *A. brevis*, *A. alleni*, *A. subequatorius*, and *A. philippinensis* ~~is not studied so far.~~ Likewise, the prodissoconch of *A. croulensis*, which is smooth and lacks sculpture, was not examined with a scanning microscope (*Oliver & Killeen, 2002*). Perhaps, the prodissoconch of all the above species has an external sculpture that can be distinguished only at high magnification using scanning microscopy. It cannot be ruled out that further examination of the prodissoconch of these species will reveal more morphological features, allowing a more accurate diagnosis of largely morphologically similar species of the genus *Axinulus*.

Acknowledgments

I am very grateful to Drs. A.V. Gebruk, E.M. Krylova, all staff of the Laboratory of Ocean Bottom Fauna (IO RAS), as well as to Drs. H. Saito (NMNS), P. Valentich-Scott (SBMNH), and L.T. Groves (LACM) for arrangement of my work with the bivalve mollusk collections and great

help during this research; to Dr. H. Saito (NMNS) for the photographs of paratypes and additional material of *A. obliqua*; to Dr. O.V. Yurchenko (NSCMB FEB RAS) for making preparations and photos of the eggs of *A. krylovae* sp. nov.; Prof. Dr. A. Brandt (Senckenberg Research Institute and Natural History Museum, and Goethe University Frankfurt, Frankfurt), chief scientist of the KuramBio and KuramBio II expeditions, and to Dr. M.V. Malyutina (NSCMB FEB RAS), chief scientist of the SokhoBio expedition and coordinator of the Russian team of the KuramBio and KuramBio II expeditions, for invitation to join the deep-sea expeditions, and to the scientific staff of the expeditions and the ship crews for their assistance during the expeditions; to Ms. T.N. Koznova (NSCMB FEB RAS) for help with the translation of the manuscript into English.

References

Allen JA. 2008. Bivalvia of the deep Atlantic. *Malacologia* 50(1):57-173 https://doi.org/10.4002/0076-2997-50.1.57

Allen JA. 2015. Bivalves collected from the bottom of the Philippine Trench, including a new species of *Axinulus* (Thyasiroidea). *Journal of Conchology* 42(2):175-182

Belyaev GM. 1989. *Deep-sea oceanic trenches and their fauna.* Moscow: Nauka Press (in Russian)

Belyaev GM, Mironov AN. 1977. Bottom fauna of the West Pacific deep-sea trenches. *Proceedings of P.P. Shirshov Institute of Oceanology* 108:7-24 (in Russian)

Brandt A, Malyutina MV. 2015. The German-Russian deep-sea expedition KuramBio (Kurile Kamchatka biodiversity studies) on board of RV Sonne in 2012 following the footsteps of the legendary expeditions with RV Vityaz. *Deep-Sea Research Part II: Topical Studies in Oceanography* 111:1-9 https://doi.org/10.1016/j.dsr2.2014.11.001

553 Brandt A, Elsner NO, Brenke N, Golovan OA, Malytina MV, Riehl T, Schwabe E, Würzberg L.
554 2013. Epifauna of the Sea of Japan collected via a new epibenthic sledge equipped with
555 camera and environmental sensor systems. *Deep-Sea Research Part II: Topical Studies in*
556 *Oceanography* 86-87:43-55
557 Brandt A, Elsner NO, Malytina MV, Brenke N, Błażewicz M, Golovan OA, Lavrenteva AV,
558 Riehl T. 2015. Abyssal macrofauna of the Kuril-Kamchatka Trench area (Northwest Pacific)
559 collected by means of a camera-epibenthic sledge. *Deep-Sea Research Part II: Topical*
560 *Studies in Oceanography* 111:175-187 https://doi.org/10.1016/j.dsr2.2014.11.002
561 Brandt A, Alalykina I, Fukumori H, Golovan OA, Kniesz K, Lavrenteva AV, Lörz AN,
562 Malyutina MV, Philipps-Bussau K, Stransky B. 2018. First insights into macrofaunal
563 composition from the SokhoBio expedition (Sea of Okhotsk, Bussol Strait and northern
564 slope of the Kuril-Kamchatka Trench). *Deep-Sea Research Part II: Topical Studies in*
565 *Oceanography* 154:106-120 https://doi.org/10.1016/j.pocean.2019.102131
566 Brandt A, Alalykina I, Brix S, Brenke N, Błażewicz M, Golovan OA, Johannsen N, Hrinko AM,
567 Jażdżewska AM, Jeskulke K, Kamenev GM, Lavrenteva AV, Malyutina MV, Riehl T, Lins
568 L. 2019. Depth zonation of Northwest Pacific deep-sea macrofauna. *Progress in*
569 *Oceanography* 176:102131
570 Brandt A, Brix S, Riehl T, Malyutina M. 2020. Biodiversity and biogeography of the abyssal and
571 hadal Kuril-Kamchatka trench and adjacent NW Pacific deep-sea regions. *Progress in*
572 *Oceanography* 181:102232 https://doi.org/10.1016/j.pocean.2019.102232
573 Carrozza F. 1981. Thyasira alleni n. sp. *Bollettino Malacologico* 17(9–10):223-228

574 Fujikura K, Kojima S, Tamaki K, Maki Y, Hunt J, Okutani T. 1999. The deepest
575 chemosynthesis-based community yet discovered from the hadal zone, 7326 m deep, in the
576 Japan Trench. *Marine Ecology Progress Series* 190:17-26
577 Fujikura K, Fujiwara Y, Kojima S, Okutani T. 2002. Micro-scale distribution of mollusks
578 occurring in deep-sea chemosynthesis-based communities in the Japan Trench. *Venus*
579 60:225-236 https://doi.org/10.18941/venus.60.4_225
580 Hedley C. 1907. The Results of deep-sea investigation in the Tasman Sea. II The Expedition of
581 the "Woy Woy". *Records of the Australian Museum* 6:356-364
582 Iredale T. 1930. More notes on the marine Mollusca of New South Wales. *Records of the*
583 *Australian Museum* 17(9):384-407
584 Kamenev GM. 2013. Species composition and distribution of bivalves in bathyal and abyssal
585 depths of the Sea of Japan. *Deep-Sea Research Part II: Topical Studies in Oceanography*
586 86–87:124-139 https://doi.org/10.1016/j.dsr2.2012.08.004
587 Kamenev GM. 2014. Two new species of the genus *Silicula* (Bivalvia: Siliculidae) from the
588 northwestern Pacific, with notes on *Silicula sandersi* (Bernard, 1989) and *Propeleda*
589 *soyomaruae* (Okutani, 1962). *Malacologia* 57:255-277 https://doi.org/10.4002/040.057.0201
590 Kamenev GM. 2015. Composition and distribution of bivalves of the abyssal plain adjacent to
591 the Kuril-Kamchatka Trench (Pacific Ocean). *Deep-Sea Research Part II: Topical Studies in*
592 *Oceanography* 111:188-197 https://doi.org/10.1016/j.dsr2.2014.08.005
593 Kamenev GM. 2018a. Bivalve molluscs of the abyssal zone of the Sea of Okhotsk: species
594 composition, taxonomic remarks, and comparison with the abyssal fauna of the Pacific
595 Ocean. *Deep-Sea Research Part II: Topical Studies in Oceanography* 154:230-248
596 https://doi.org/10.1016/j.dsr2.2017.10.006

Kamenev GM. 2018b. Four new species of the family Propeamussiidae (Mollusca: Bivalvia) from the abyssal zone of the northwestern Pacific, with notes on *Catillopecten squamiformis* (Bernard, 1978). *Marine Biodiversity* 48:647-676 https://doi.org/10.1007/s12526-017-0821-1

Kamenev GM. 2018c. Three new species of the genus *Hyalopecten* (Bivalvia: Pectinidae) from the abyssal and hadal zones of the North-western Pacific Ocean. *Journal of the Marine Biological Association of the United Kingdom* 98(2):357-374

Kamenev GM. 2019. Bivalve mollusks of the Kuril-Kamchatka Trench, Northwest Pacific Ocean: species composition, distribution and taxonomic remarks. *Progress in Oceanography* 176:102127 https://doi.org/10.1016/j.pocean.2019.102127

Kamenev GM. 2020. Three new deep-sea species of Thyasiridae (Mollusca: Bivalvia) from the abyssal plain of the northwestern Pacific Ocean and hadal depths of the Kuril-Kamchatka Trench. *PeerJ* 8:e10405 https://doi.org/10.7717/peerj.10405

Kamenev GM. 2023. Three new deep-sea species of Thyasiridae (Mollusca: Bivalvia) from the northwestern Pacific Ocean. *European Journal of Taxonomy* 856(1):87-119 https://doi.org/10.5852/ejt.2023.856.2031

Kamenev GM, Mordukhovich VV, Alalykina IL, Chernyshev AV, Maiorova AS. 2022. Macrofauna and nematode abundance in the abyssal and hadal zones of interconnected deep-sea ecosystems in the Kuril Basin (Sea of Okhotsk) and the Kuril-Kamchatka Trench (Pacific Ocean). *Frontiers in Marine Science* 9:812464 https://doi.org/10.3389/fmars.2022.812464

Knudsen J. 1970. The systematic and biology of abyssal and hadal Bivalvia. *Galathea Report* 11:1-238

620 Malyutina MV, Brandt A. 2013. Introduction to SoJaBio (Sea of Japan Biodiversity Studies).
621 *Deep-Sea Research Part II: Topical Studies in Oceanography* 86–87:1-9
622 https://doi.org/10.1016/j.dsr2.2012.08.011
623 Malyutina MV, Chernyshev AV, Brandt A. 2018. Introduction to the SokhoBio (Sea of Okhotsk
624 Biodiversity Studies) expedition 2015. *Deep-Sea Research Part II: Topical Studies in*
625 *Oceanography* 154:1-9 https://doi.org/10.1016/j.dsr2.2018.08.012
626 Monin AS. (ed.) 1983. *Research Vessel "Vityaz" and his Expeditions 1949–1979.* Moscow:
627 Nauka Press (in Russian)
628 Okutani T. 1974. Review and new records of abyssal and hadal molluscan fauna in Japanese and
629 adjacent waters. *Venus* 33:23-39
630 Okutani T. 2000. *Marine molluscs in Japan.* Tokyo: Tokai University Press
631 Okutani T. 2003. Review of Benthic Molluscan fauna in the Japan Trench. *Japanese Journal of*
632 *Benthology* 58:40-43
633 Okutani T, Fujikura Y. 2002. Abyssal gastropoda and bivalves collected by Shinkai 6500 on
634 slope of the Japan Trench. *Venus* 60:211-224
635 Okutani T, Fujikura K, Kojima S. 1999. Two new hadal bivalves of the family Thyasiridae from
636 the plate convergent area of the Japan Trench. *Venus* 58:49-54
637 Okutani T, Fujiwara Y. 2005. Four protobranch bivalves collected by the ROV *Kaiko* from hadal
638 depths in the Japan Trench. *Venus* 63:87-94
639 Okutani T, Kawamura R. 2002. Abyssal bivalves collected from beyond 3,000 m in the
640 Northwestern Pacific and Shikoku Basins by the R/V *Soyo-Maru,* 1977-1981. *Bulletin of the*
641 *National Museum of Nature and Science. Series A (Zoology)* 28:1-19

642 Oliver PG. 2015. Deep-water Thyasiridae (Mollusca: Bivalvia) from the Oman Margin, Arabian
643 Sea, new species and examples of endemism and cosmopolitanism. *Zootaxa* 3995(1):252-
644 263 https://doi.org/10.11646/zootaxa.3995.1.21
645 Oliver PG, Killeen IJ. 2002. The Thyasiridae (Mollusca: Bivalvia) of the British Continental
646 Shelf and North Sea oil fields: an identification manual. *Studies in Marine Biodiversity and*
647 *Systematics from the National Museum of Wales. BIOMÔR Reports* 3:1-73
648 Oliver PG, Levin L. 2006. A new species of the family Thyasiridae (Mollusca: Bivalvia) from
649 the oxigen minimum zone of the Pakistan margin. *Journal of the Marine Biological*
650 *Association of the United Kingdom* 86(2):411-416
651 Payne CM, Allen JA. 1991. The morphology of deep sea Thyasiridae (Mollusca: Bivalvia) from
652 the Atlantic Ocean. *Philosophical Transactions of the Royal Society, Series B*
653 334(1272):481-562 https://doi.org/10.1098/rstb.1991.0128
654 Verrill AE, Bush KJ. 1898. Revision of the deep-water Mollusca of the Atlantic coast of North
655 America, with descriptions of new genera and species. *Part. I. Bivalvia. Proceedings of the*
656 *United States National Museum* 20(1139):775-901 https://doi.org/10.5479/si.00963801.20-
657 1139.775
658 WoRMS Editorial Board. 2023. World register of marine species. https://doi.org/10.14284/170
659 Zelaya DG. 2009. The genera *Thyasira* and *Parathyasira* in the Magellan region and adjacent
660 Antarctic waters (Bivalvia: Thyasiridae). *Malacologia* 51(2):271-290
661 https://doi.org/10.4002/040.051.0204
662 Zelaya DG. 2010. New species of *Thyasira*, *Mendicula*, and *Axinulus* (Bivalvia, Thyasiroidea)
663 from Sub-Antarctic and Antarctic waters. *Polar Biology* 33(5):607-616
664 https://doi.org/10.1007/s00300-009-0736-9

Figure 1

Placement of shell measurements.

Placement of shell measurements. Abbreviations: L, shell length; H, height; A, anterior end length; W, shell width.

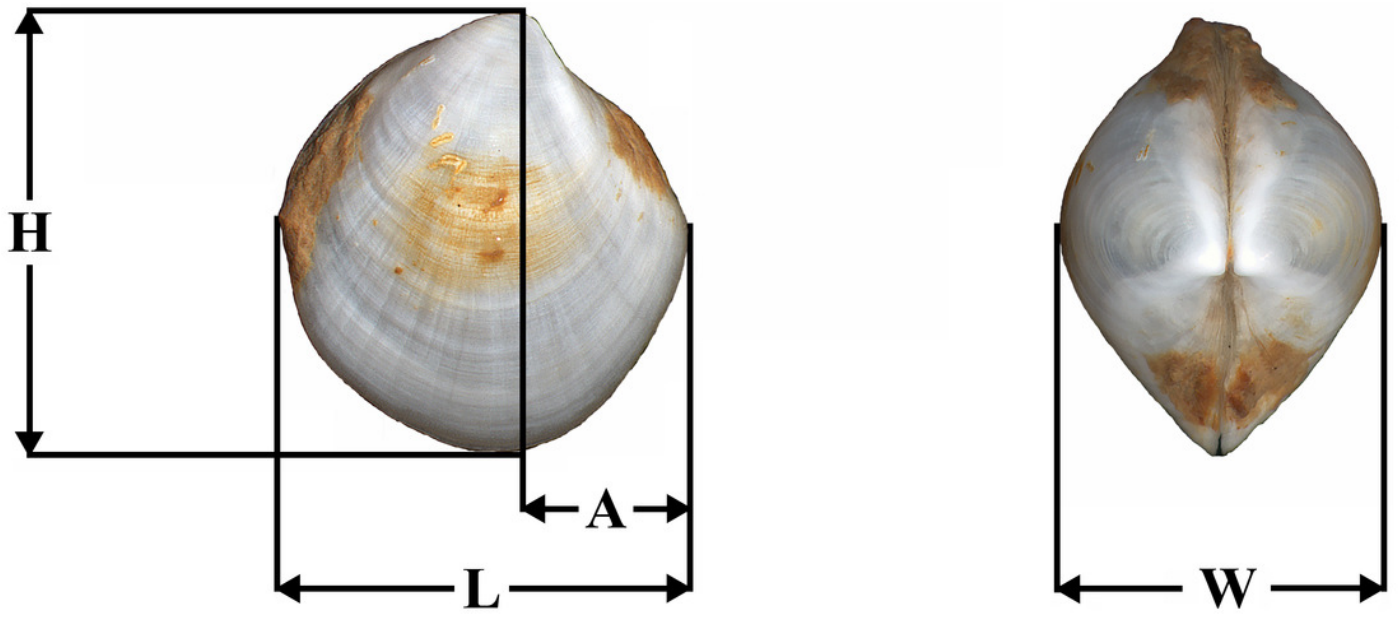

Figure 2

Axinulus krylovae sp. nov.

Axinulus krylovae sp. nov. (A-D) Holotype (IORAS XXXXX), exterior and dorsal views, and sculpture of central shell part, shell length 4.9 mm. (E and F) Paratype (IORAS XXXXX), exterior and oblique dorsal views, shell length 5.0 mm. (G and J) Exterior and interior views of right and left valves, and hinge plates of both valves, valves length 4.4 mm. (K-M) Variability of shell shape, exterior view of right valves of specimens from holotype locality: (K) Shell length 3.5 mm ; (L) Shell length 4.3 mm; (M) Shell length 4.0 mm. Scale bar: I, J = 1 mm.

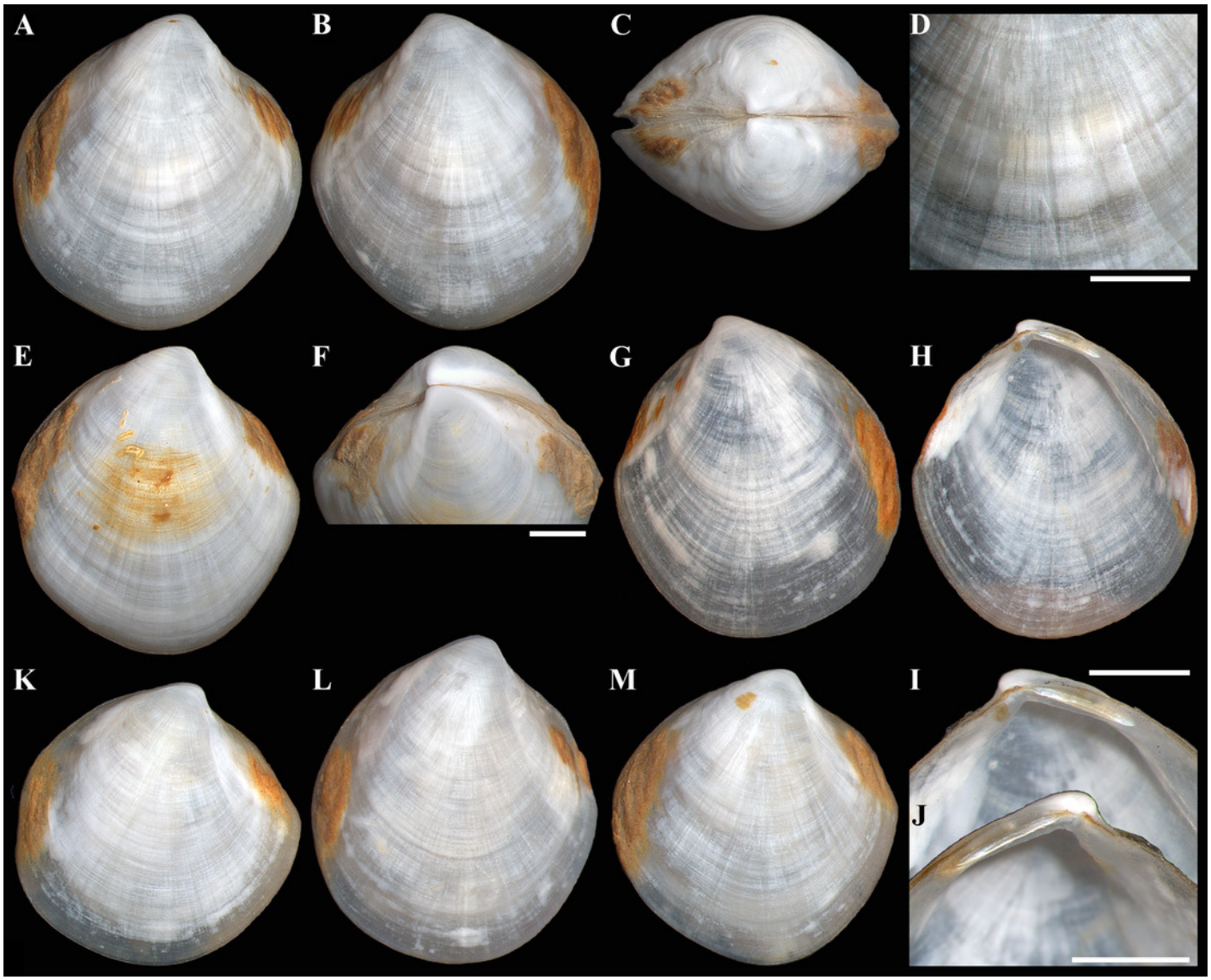
A
B
C
D
E
F
G
H
K
L
M
I
J

Figure 3

Scanning electron micrographs of *Axinulus krylovae* sp. nov.

(A) Dorsal view of both valves. (B) Dorsal view of posterodorsal margin. (C) Lunule. (D) Oblique dorsal view of lunule. (E-H) Specimen from the Japan Trench, depth 7,540 m: (E) Exterior view of right valve. (F) Sculpture of beak region. (G and H) Sculpture of central shell part. (I-L) Specimen from the Kuril-Kamchatka Trench, depth 8,734 m: (I) Exterior view of right valve. (J) Sculpture of beak region. (K) Sculpture of ventral shell part. (L) Sculpture of central shell part. (M-P) Sculpture of anterior shell end. (F, G) Sculpture of posterior shell end. (H) Interior view of left valve. (I) Hinge plate and ligamental groove of left valve. (J, K) Ventral view of hinge plate and ligamental groove of left valve. (L) Interior view of right valve. (M-P) Prodissoconch of specimen from the Japan Trench. (Q-T) Prodissoconch of specimen from the Kuril-Kamchatka Trench. Scale bars: A, C-E, J = 1 mm; F-H, J-L, = 100 µm; M-T = 10 µm.

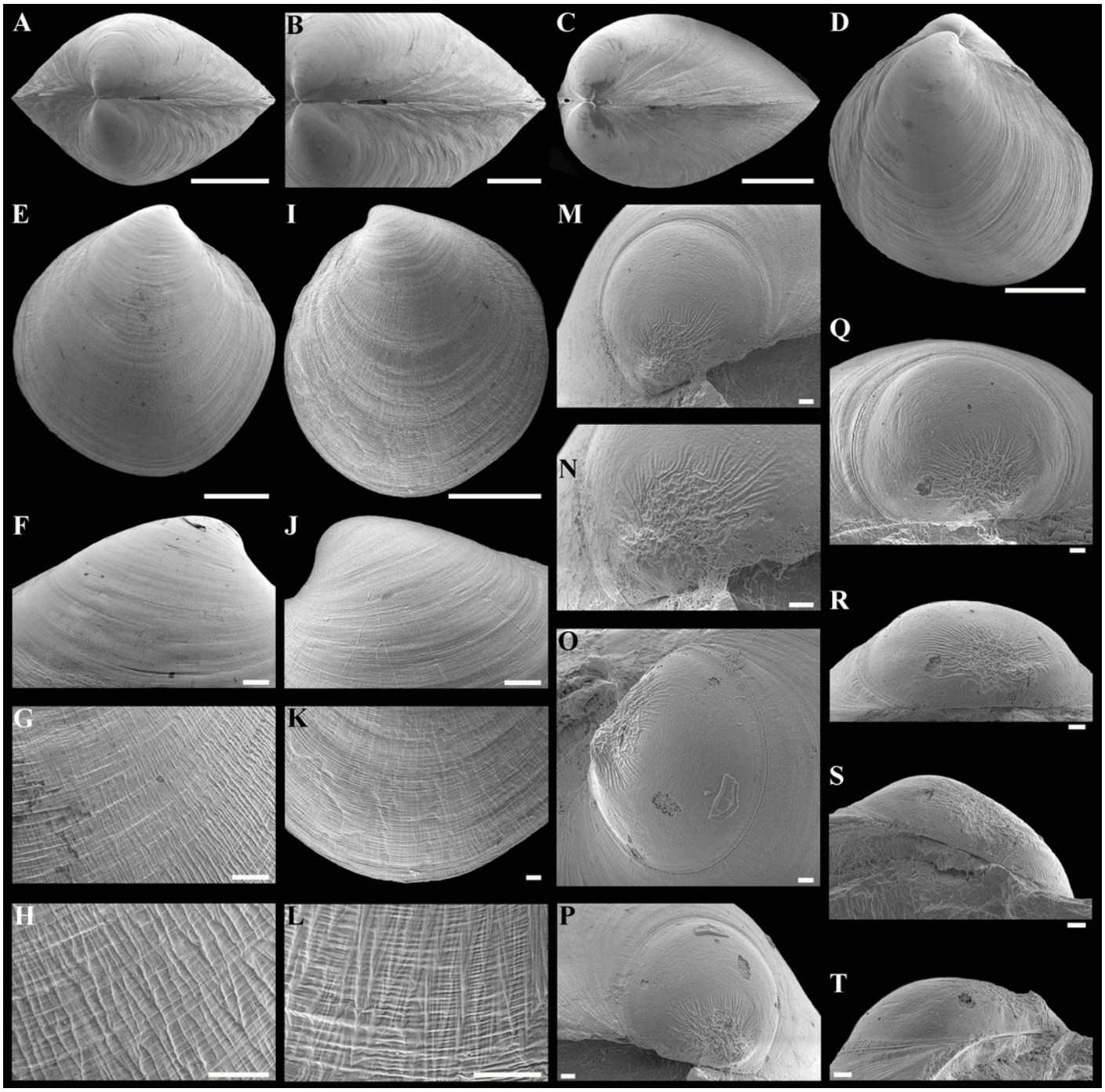
A
B
C
D
E
I
M
Q
N
F
J
R
O
G
K
S
H
L
P
T

Figure 4

Scanning electron micrographs of *Axinulus krylovae* sp. nov.

Scanning electron micrographs of *Axinulus krylovae* sp. nov. (A-H) Specimen from the Kuril-Kamchatka Trench, depth 8,700 m: (A and B) Interior and ventral views of right valve. (C and D) Hinge plate and ligamental groove of right valve. (E and F) Interior and ventral views of left valve. (G and H) Hinge plate and ligamental groove of left valve. (I-P) Specimen from the Japan Trench, depth 7,540 m: (I and J) Interior and ventral views of right valve. (K and L) Hinge plate and ligamental groove of right valve. (M and N) Interior and ventral views of left valve. (O and P) Hinge plate and ligamental groove of left valve. (Q-T) Exterior and interior views of valves of young specimens: (Q and R) Specimen from the Kuril-Kamchatka Trench, depth of 8,700 m. (S and T) Specimen from the abyssal plain adjacent to the Kuril-Kamchatka Trench, depth of 5,125 m. Scale bars: A, B, E, F, I, J, M, N, Q, R = 500 µm; C, D, G, H, K, L, O, P, S, T = 100 µm.

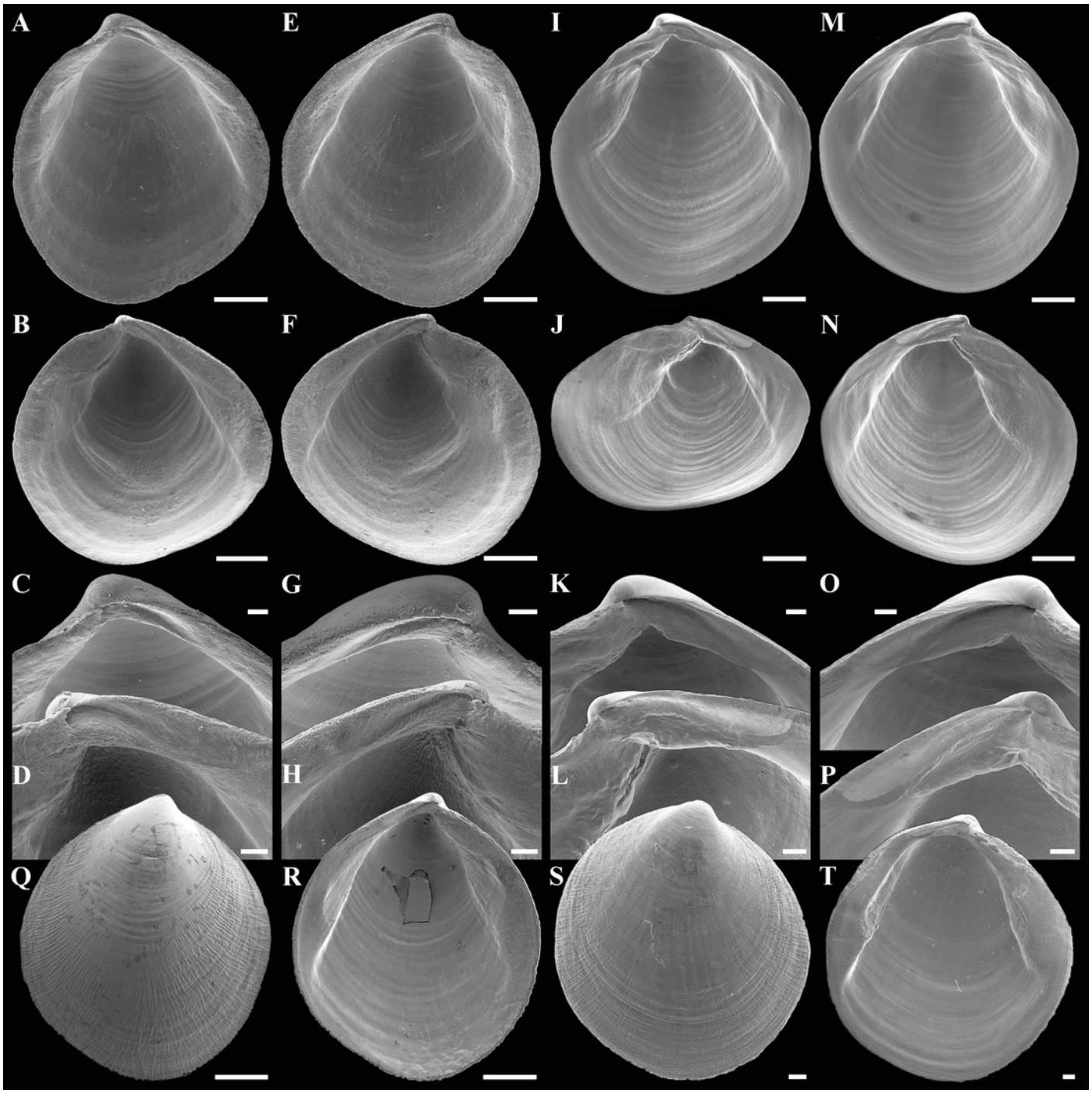
A
E
I
M
B
F
J
N
C
G
K
O
D
H
L
P
Q
R
S
T

Figure 5

Axinulus krylovae sp. nov.

Axinulus krylovae sp. nov. (A) Exhalant apertures. (B) Gross anatomy after removal of right valve and mantle. (C) Gross anatomy after further removal of right ctenidium. (D and E) Gross anatomy after further removal of right lateral body pouch. (F) Labial palps, anterior pedal and adductor muscles. (G) Gross anatomy after further removal of right kidney. (H) Kidney with orange granules. (I) Digestive system. (J) Posterior view of kidneys, ctenidium, and lateral body pouches of live specimen after removal shell and mantle. (K) Foot of live specimen. (L) Egg (photo by Dr. O.V. Yurchenko (NSCMB FEB RAS)). (M) Gross anatomy after removal of right valve, mantle, right kidney, and posterior adductor muscle. (N) Gross anatomy after further removal of right ctenidium and mantle edge. (O) Gross anatomy after further removal of right lateral body pouch and anterior adductor muscle. (P) Digestive system. Abbreviations: AA, anterior adductor muscle; APR, anterior pedal retractor muscle; EA, exhalant aperture; F, foot; HG, hind gut; ID, inner demibranch; K, kidney; L, ligament; LBP, lateral body pouch; LP, labial palps; ME, mantle edge; MG, mid gut; NP, neck of lateral body pouch; PA, posterior adductor muscle; PPR, posterior pedal retractor muscle; S, stomach. Scale bars: A-K, M-P = 1 mm; L = 100 µm .

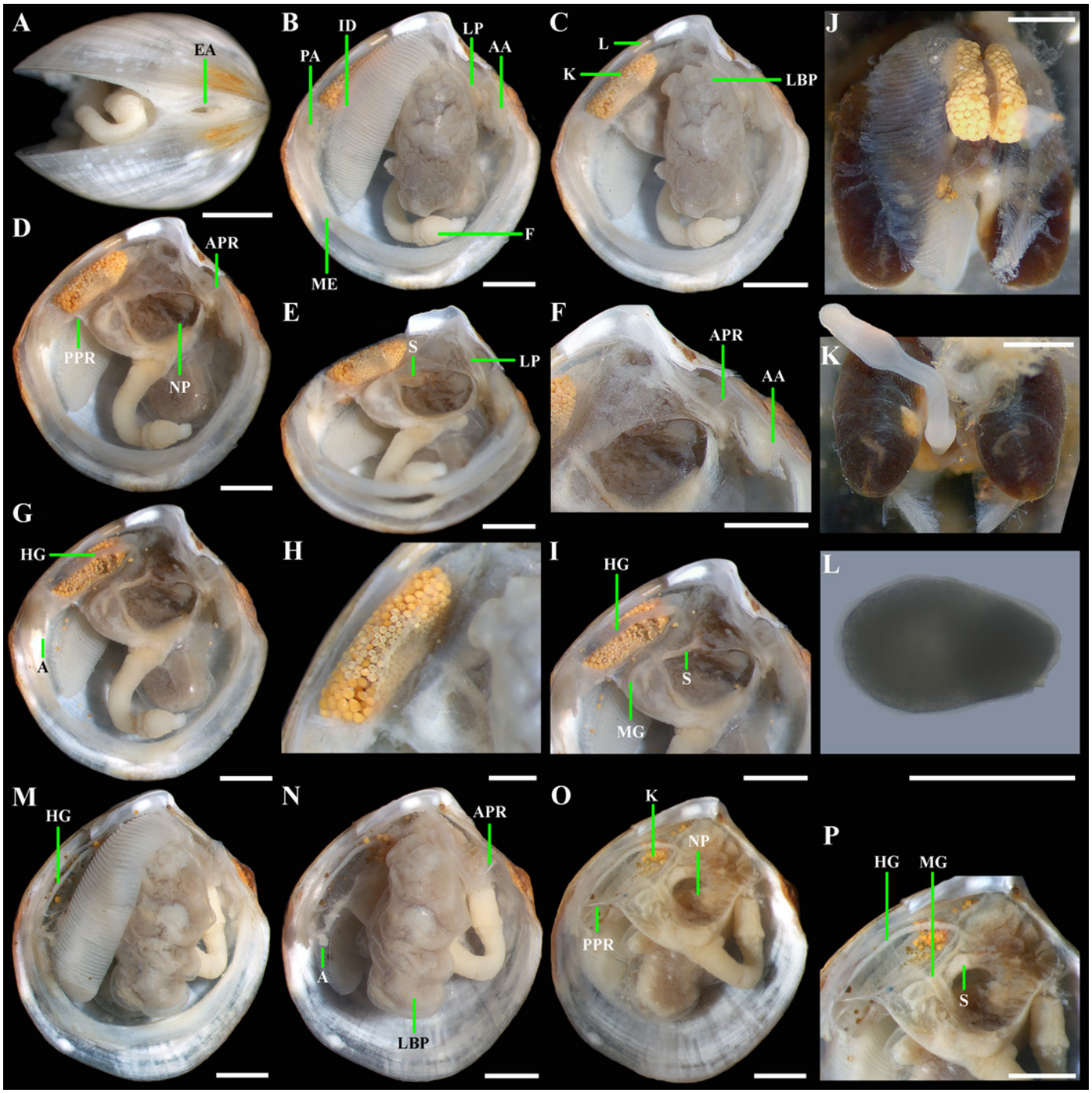
A
EA
B
ID
PA
LP
AA
F
ME
C
L
K
LBP
J
D
APR
PPR
NP
E
S
LP
F
APR
AA
K
G
HG
A
H
I
HG
S
MG
L
M
HG
N
APR
A
LBP
O
K
NP
PPR
P
HG
MG
S

Figure 6

Axinulus alatus sp. nov.

Axinulus alatus sp. nov. (A-D) Holotype (MIMB XXXXX), exterior, dorsal, and oblique dorsal views of both valves, shell length 2.4 mm. (E and F) Interior view and hinge plate of right valve, valve length 2.7 mm. (G) Paratype (MIMB XXXXX), exterior view of right valve, shell length 2.7 mm. (G and I) Paratype (ZMF XXXXX), exterior view of right valve and dorsal view of both valves, shell length 2.3 mm. (J-M) Variability of shell shape, exterior view of right valves: (J) Shell length 1.7 mm; (K) Shell length 2.5 mm ; (L) Shell length 1.5 mm; (M) Shell length 2.1 mm. Scale bar: F = 500 µm.

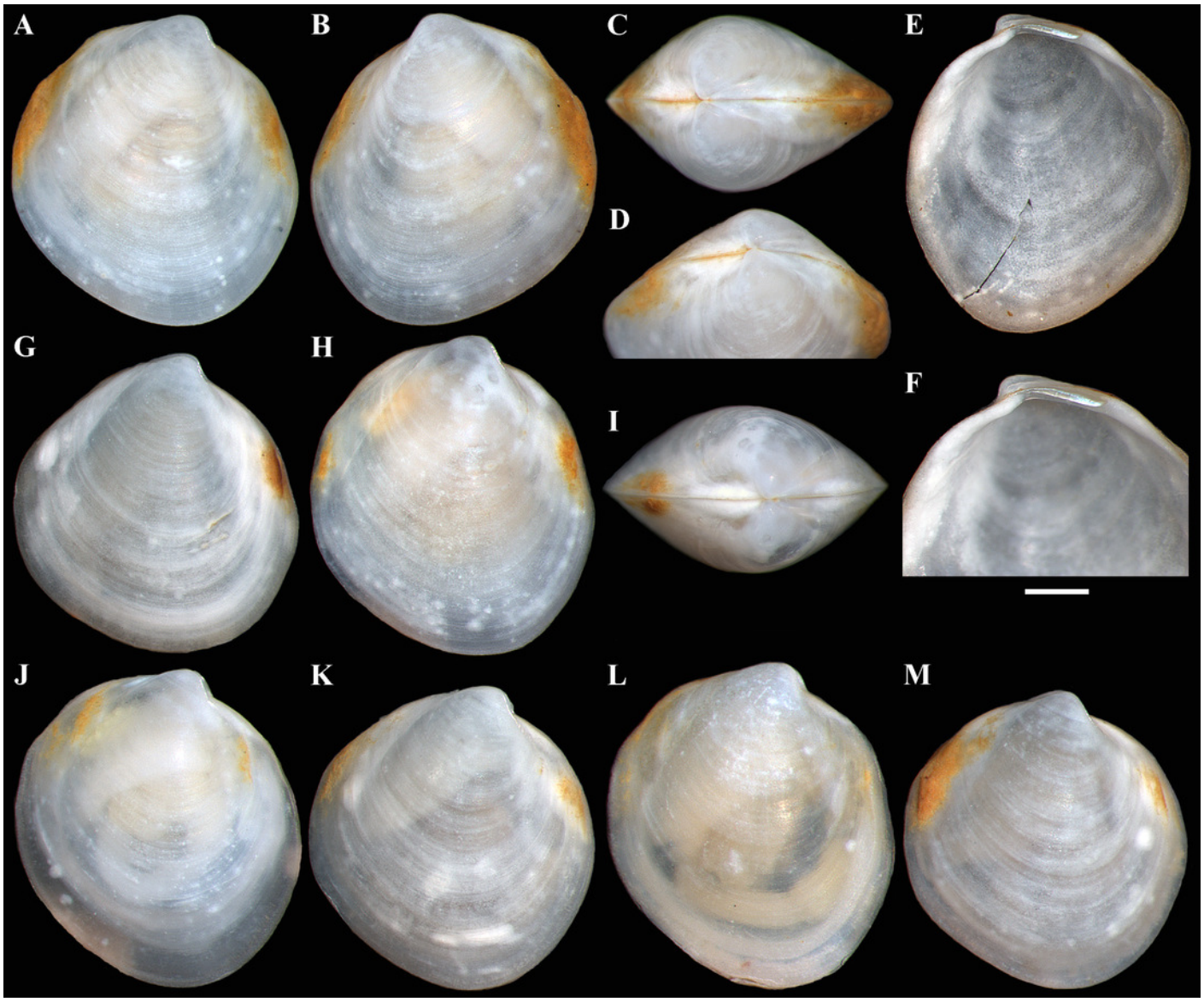
A
B
C
E
D
G
H
F
I
J
K
L
M

Figure 7

Scanning electron micrographs of *Axinulus alatus* sp. nov.

Scanning electron micrographs of *Axinulus alatus* sp. nov. (A) Dorsal view of both valves. (B and C) Escutcheon. (D) Lunule. (E) Exterior view of left valve. (F) Sculpture of beak region. (G) Posterodorsal margin of left valve with auricle. (H) Sculpture of ventil shell part. (I and J) Sculpture of central shell part. (K) Interior view of right valve. (I) Hinge plate and ligamental groove of right valve. (M, N) Ventral view of hinge plate and ligamental groove of right valve. (O) Interior view of left valve. (P) Hinge plate and ligamental groove of left valve. (Q and R) Ventral view of hinge plate and ligamental groove of left valve. Scale bars: A-H, K-R = 100 µm ; I, J = 10 µm.

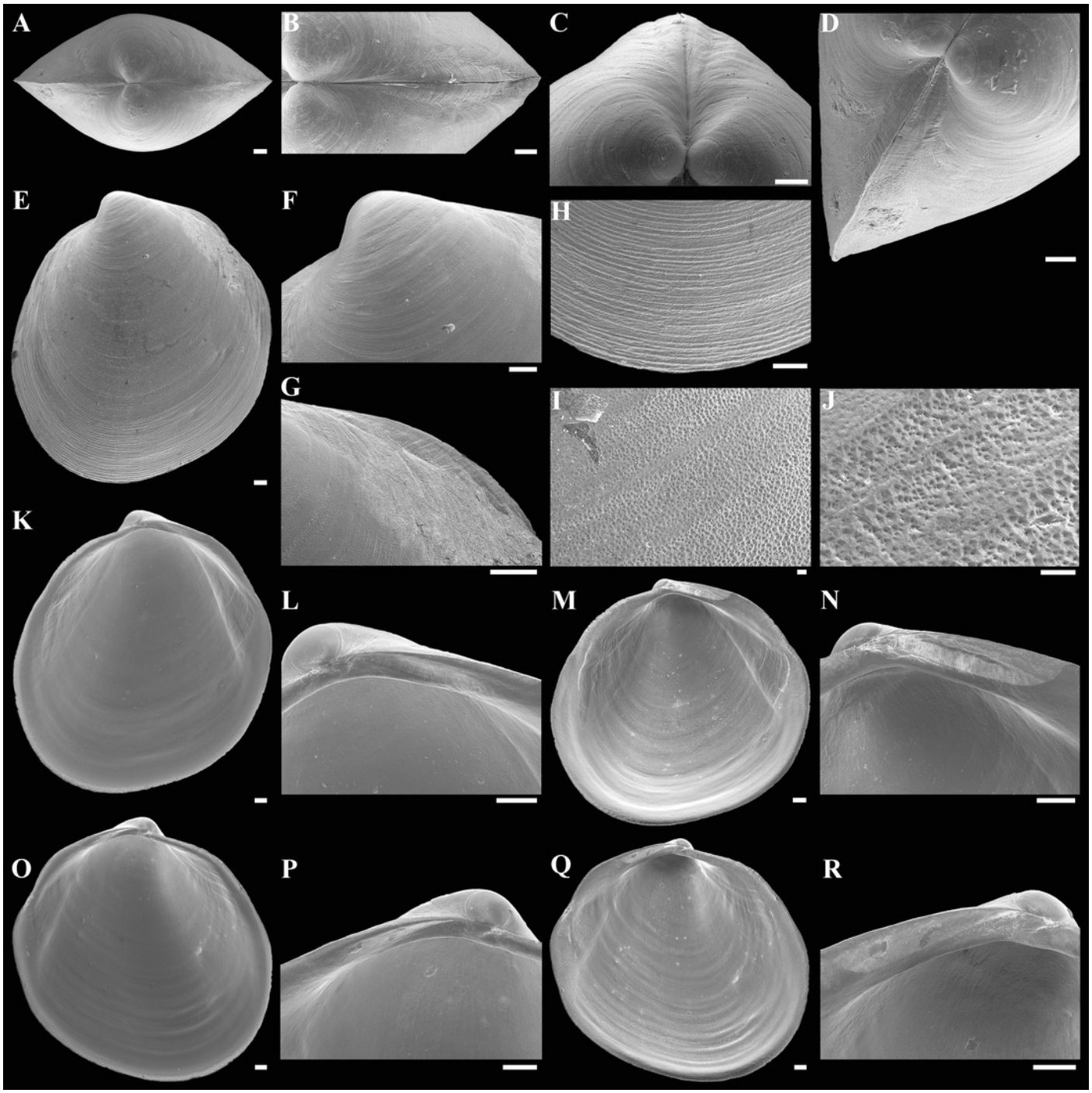
A
B
C
D
E
F
H
G
I
J
K
L
M
N
O
P
Q
R

Figure 8

Scanning electron micrographs of prodissoconchs of *Axinulus alatus* sp. nov.

Scanning electron micrographs of prodissoconchs of *Axinulus alatus* sp. nov. (A-F) Prodissoconchs of specimens from oceanic slope of the Kuril Islands, depth 3,432 m. (G and H) Prodisoconchs of specimens from the Bering Sea, depth 3,978 m. Scale bars: A-H = 50 µm

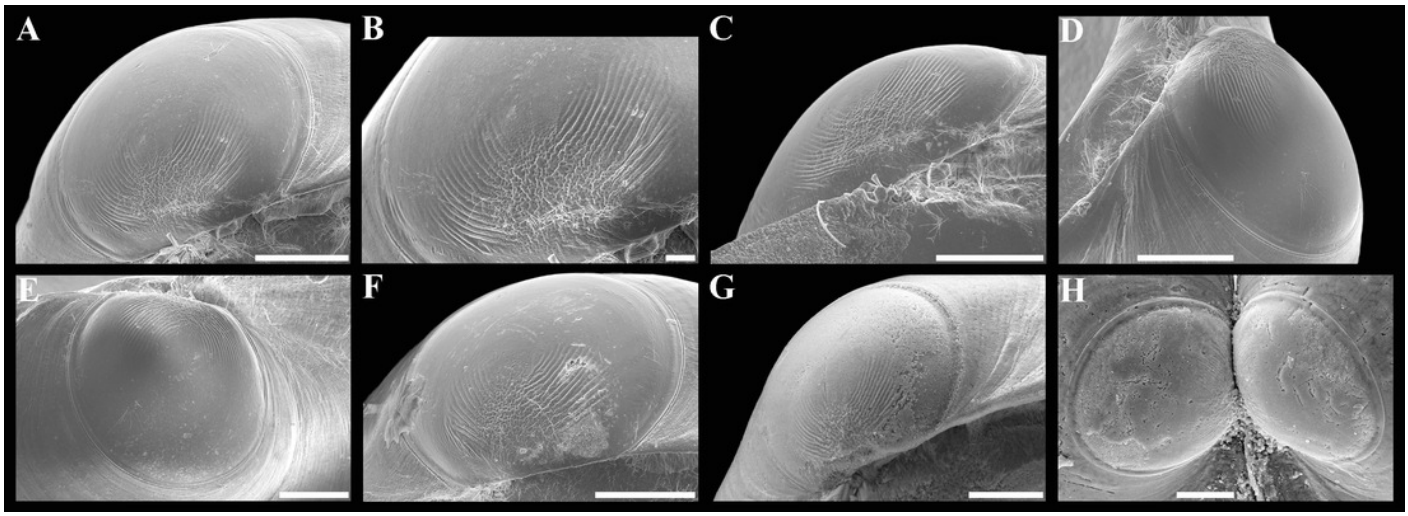

Figure 9

Axinulus alatus sp. nov.

Axinulus alatus sp. nov. (A) Exhalant apertures. (B) Gross anatomy after removal of right valve and mantle. (C) Gross anatomy after further removal of right ctenidium. (D) Gross anatomy after further removal of right lateral body pouch. (E) Digestive system. (F) Gross anatomy after removal of right valve, mantle, right ctenidium, and bulbous portion of foot. (G) Gross anatomy after further removal of right lateral body pouch and mantle edge. (H) Digestive system. Abbreviations: AA, anterior adductor muscle; APR, anterior pedal retractor muscle; EA, exhalant aperture; F, foot; HG, hind gut; ID, inner demibranch; K, kidney; L, ligament; LBP, lateral body pouch; LP, labial palps; ME, mantle edge; MG, mid gut; NP, neck of lateral body pouch; PA, posterior adductor muscle; PPR, posterior pedal retractor muscle; S, stomach. Scale bars: A-H = 500 µm.

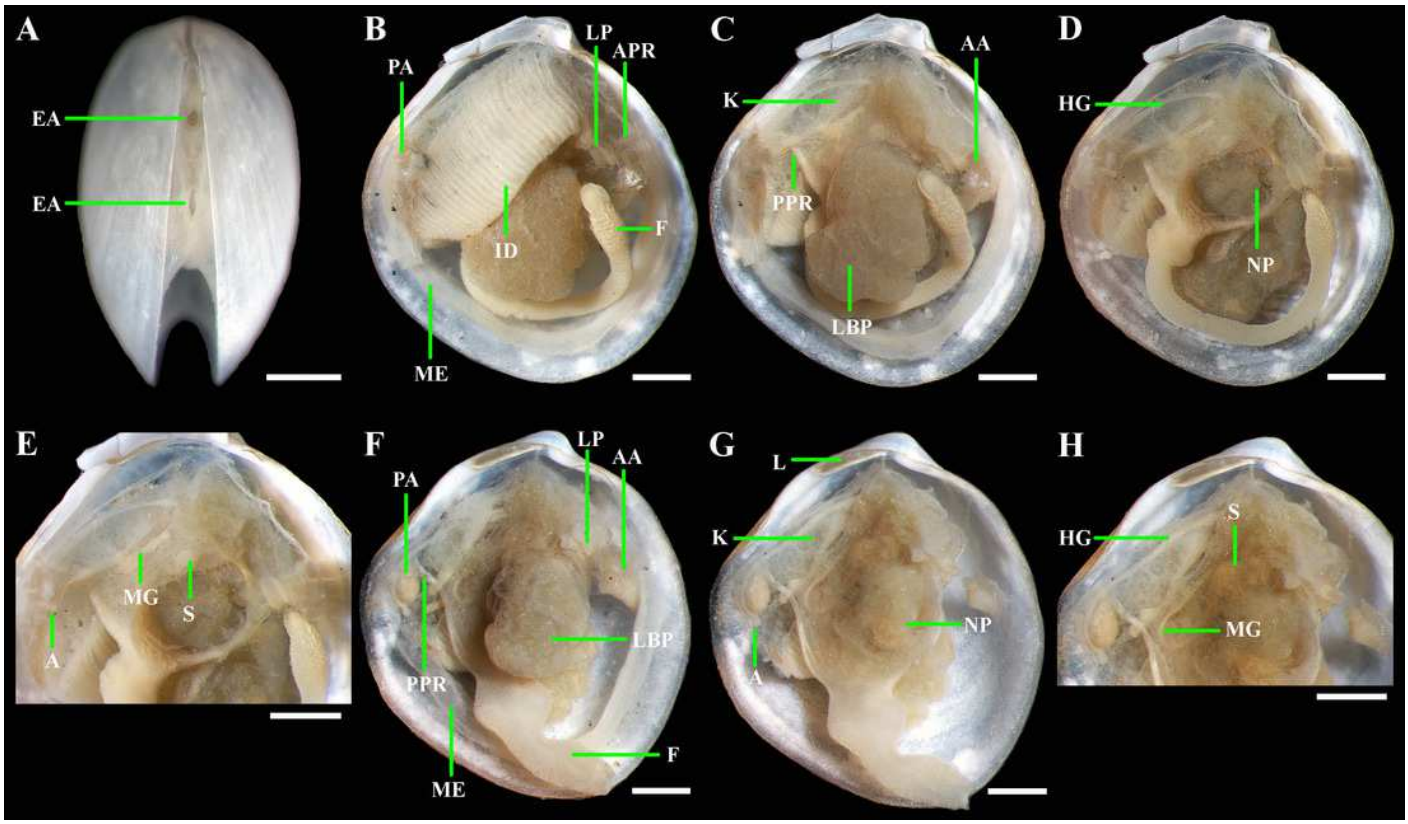

Figure 10

Scanning electron micrographs of the holotype of *Axinulus cristatus* sp. nov. (MIMB XXXXX).

Scanning electron micrographs of the holotype of *Axinulus cristatus* sp. nov. (MIMB XXXXX). (A) Exterior view of right valve. (B-D) Sculpture of ventral shell part. (E) Interior view of left valve. (F) Ventral view of left valve. (G) Hinge plate and ligamental groove of left valve. (H and I) Spoon-shaped tubercle under beak in left valve. (J-M) Prodissoconch. Scale bars: A, E, F = 500 µm; B, G, H = 100 µm; C, I, J-M = 50 µm; D = 10 µm.

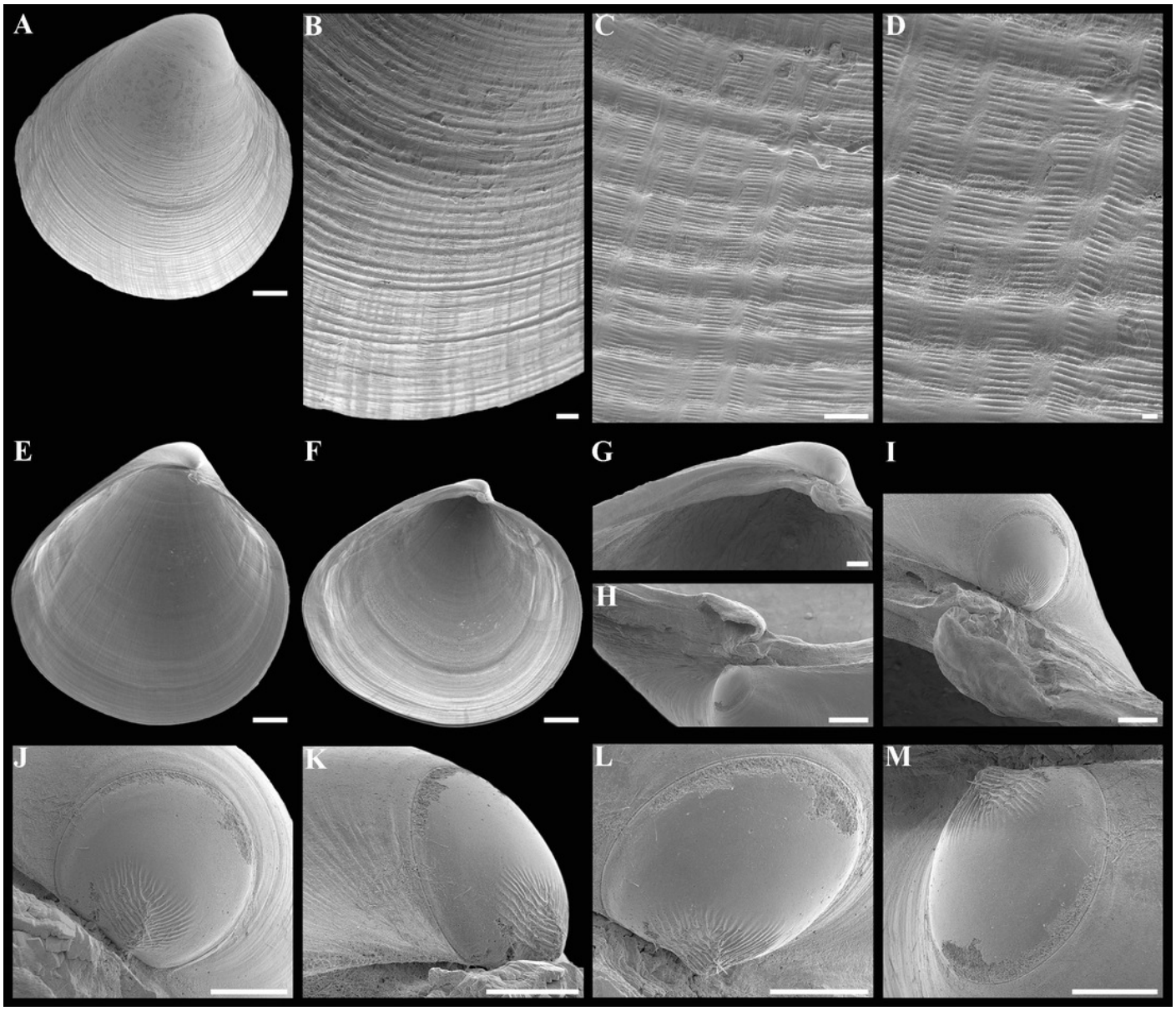
A
B
C
D
E
F
G
H
I
J
K
L
M

Table 1(on next page)

Additional material of *Axinulus krylovae* sp. nov. examined in the present study.

GT, Galathea trawl, OG, Okean grab (0.25 m^2), ST, Sigsbee trawl, GKG, giant box corer (0.25 m^2) , EBS, epibenthic sledge, AGT, Agassiz trawl, *N*, number of live specimens.

Ship, cruise no.	Station	Date	Start		End		Depth (m)	Gear	*N*	Depository
			Latitude ºN	Longitude ºE	Latitude ºN	Longitude ºE				
					Japan Trench					
Vityaz 45	6151	28.06.1969	37°41.5′	143°54.3′	-	-	7,370	ST	1	IORASXX
Vityaz 59	7500	21.06.1976	37°38'	143°58'	-	-	7,370-7,350	GT	1	IORASXX
	7503	23.06.1976	36°44'	143°19'	-	-	7,540	GT	74	IORASXX
	7511	27.06.1976	38°38'	144°06'	-	-	7,500	OG	1	IORASXX
					Kuril-Kamchatka Trench					
Vityaz 19	3168	04.10.1954	45°41.7'	152°36.7'	-	-	6,150	OG	8	IORASXX
Vityaz 39	5615	03.08.1966	45°56'	153°28'	-	-	8,060-8,135	ST	2	IORASXX
Sonne 223	17	22.08.2016	45°51.514'	153°50.581'	45°51.401'	153°50.406'	8,183-8,184	EBS	6	MIMBXXX
	19	23.08.2016	45°51.566'	153°50.451'	45°51.412'	153°50.215'	8,189-8,187	EBS	2	MIMBXXX
	25	25.08.2016	45°55.235'	152°47.464'	-	-	6,068	GKG	3	MIMBXXX
	28	26.08.2016	45°53.959'	152°45.838'	45°54.520'	152°47.204'	6,087-6,047	EBS	1	MIMBXXX
	29	26.08.2016	45°56.587'	152°54.251'	45°56.570'	152°54.499'	6,204-6,202	AGT	2	MIMBXXX
	30	27.08.2016	45°56.821'	152°51.185'	45°56.834'	152°50.943'	6,168-6,164	EBS	8	MIMBXXX
	37	28.08.2016	45°38.604'	152°55.911'	-	-	7,136	GKG	1	MIMBXXX
	40	29.08.2016	45°40.686'	152°57.374'	45°40.839'	152°57.687'	7,060-7,055	EBS	1	MIMBXXX
	42	30.08.2016	45°40.173'	152°57.457'	45°40.263'	152°57.638'	7,122-7,120	EBS	6	MIMBXXX
	49	04.09.2016	45°28.752'	153°11.649'	-	-	8,739	GKG	3	MIMBXXX
	51	05.09.2016	45°28.748'	153°11.654'	-	-	8,737	MUC	1	MIMBXXX
	52	05.09.2016	45°29.347'	153°11.415'	45°29.187'	153°11.138'	8,738-8,699	EBS	24	MIMBXXX
	54	06.09.2016	45°28.139'	153°10.624'	45°28.125'	153°10.109'	8,701-8,735	AGT	14	MIMBXXX
	55	07.09.2016	45°29.491'	153°12.540'	45°29.580'	153°12.240'	8,740-8,735	EBS	11	MIMBXXX
	67	10.09.2016	45°12.944'	152°42.844'	-	-	9,495	GKG	1	MIMBXXX
	75	12.09.2016	44°39.883'	151°28.136'	-	-	8,221	GKG	9	MIMBXXX
	77	13.09.2016	45°13.892'	152°50.774'	45°14.219'	152°49.956'	9,577-9,583	EBS	11	MIMBXXX
	89	16.09.2016	44°39.325'	151°27.340'	44°39.053'	151°27.343'	8,215-8,217	EBS	8	MIMBXXX

	90	17.09.2016	44°41.759'	151°26.554'	44°41.992'	151°26.321'	8,271-8,273	AGT	24	MIMBXXX
	94	18.09.2016	44°06.852'	151°25.539'	-	-	6,531	GKG	11	MIMBXXX
	97	18.09.2016	44°06.668'	151°24.878'	44°06.942'	151°24.888'	6,551-6,561	EBS	13	MIMBXXX
	98	19.09.2016	44°06.152'	151°25.705'	44°06.253'	151°25.935'	6,441-6,442	AGT	12	MIMBXXX
	100	20.09.2016	44°12.378'	150°39.053'	-	-	9,305	GKG	3	MIMBXXX
	103	21.09.2016	44°12.499'	150°39.055'	44°12.502'	150°37.258'	9,301-9,431	AGT	1	MIMBXXX
	105	22.09.2016	44°12.391'	150°36.006'			9,540	GKG	1	MIMBXXX
Kuril-Kamchatka Trench area and abyssal plain adjacent to trench (depth less than 6,000 m)										
Vityaz 19	3102	22.08.1954	41°16'	147°27.7'	-	-	5,210	OG	1	IORASXX
Sonne 223	1-5	29.07.2012	43°58.17'	157°19.88'	-	-	5,410	GKG	1	MIMBXXX
	2-5	02.08.2012	46°13.99'	155°33.10'	-	-	4,869	GKG	1	MIMBXXX
	2-9	02.08.2012	46°13.60'	155°33.42'	46°14.93'	155°32.57'	4,866-4,860	EBS	3	MIMBXXX
	2-11	03.08.2012	46°13.69'	155°33.29'	46°14.87'	155°32.49'	4,869-4,861	AGT	5	MIMBXXX
	3-4	04.08.2012	47°14.32'	154°42.26'	-	-	4,982	GKG	6	MIMBXXX
	3-9	05.08.2012	47°13.83'	154°41.88'	47°14.87'	154°43.18'	4,988-4,998	EBS	3	MIMBXXX
	4-4	07.08.2012	46°57.97'	154°32.49'	-	-	5,766	GKG	3	MIMBXXX
	5-4	10.08.2012	43°35.01'	153°58.09'	-	-	5,379	GKG	1	MIMBXXX
	6-4	13.08.2012	42°28.98'	153°59.97'	-	-	5,297	GKG	1	MIMBXXX
	7-4	16.08.2012	43°02.31'	152°59.16'	-	-	5,222	GKG	7	MIMBXXX
	7-5	16.08.2012	43°02.24'	152°59.09'	-	-	5,223	GKG	3	MIMBXXX
	7-9	17.08.2012	43°02.87'	152°59.45'	43°01.50'	152°58.35'	5,216-5,221	EBS	3	MIMBXXX
	7-10	17.08.2012	43°02.78'	152°59.30'	43°01.65'	152°58.45'	5,217-5,223	EBS	20	MIMBXXX
	8-4	19.08.2012	42°14.57'	151°43.51'	-	-	5,130	GKG	1	MIMBXXX
	8-5	19.08.2012	42°14.57'	151°43.51'	-	-	5,130	GKG	5	MIMBXXX
	8-9	20.08.2012	42°14.69'	151°44.05'	42°14.26'	151°42.49'	5,127	EBS	18	MIMBXXX
	8-12	21.08.2012	42°14.73'	151°44.38'	42°14.32'	151°42.94'	5,112-5,126	EBS	7	MIMBXXX
	9-5	23.08.2012	40°34.96'	151°00.07'	-	-	5,401	GKG	1	MIMBXXX
	9-9	23.08.2012	40°35.49'	150°59.92'	40°34.25'	150°59.91'	5,399-5,398	EBS	2	MIMBXXX
	9-10	24.08.2012	40°36.13'	151°00.07'	40°35.31'	151°00.12'	5,406-5,404	AGT	3	MIMBXXX
	9-12	25.08.2012	40°35.40'	150°59.84'	40°34.27'	150°59.00'	5,398	EBS	1	MIMBXXX
	10-5	26.08.2012	41°11.99'	150°05.75'	-	-	5,251	GKG	1	MIMBXXX

	10-12	27.08.2012	41°11.70'	150°05.56'	41°13.03'	150°05.71'	5,250-5,255	EBS	4	MIMBXXX
	11-4	29.08.2012	40°12.86'	148°05.92'	-	-	5,348	GKG	5	MIMBXXX
	11-9	30.08.2012	40°13.26'	148°06.24'	40°12.37'	148°05.43'	5,348-5,350	EBS	5	MIMBXXX
	11-11	30.08.2012	40°13.55'	148°06.77'	40°12.90'	148°06.20'	5,349-5,352	AGT	1	MIMBXXX
	11-12	31.08.2012	40°13.10'	148°06.45'	40°12.10'	148°05.53'	5,351-5,348	EBS	6	MIMBXXX
	12-2	31.08.2012	39°43.43'	147°09.98'	-	-	5,243	GKG	7	MIMBXXX
	12-4	01.09.2012	39°43.80'	147°10.16'	39°42.49'	147°09.37'	5,224-5,215	EBS	3	MIMBXXX
Sonne 250	6	18.08.2016	43°49.197'	151°45,609'	-	-	5,497	GKG	1	MIMBXXX
	8	19.08.2016	43°48.593'	151°46.433'	43°48.598'	151°46.477'	5,107	EBS	13	MIMBXXX
	10	20.08.2016	43°48.602'	151°47.124'	43°48.455'	151°47.171'	5,352-5,104	EBS	7	MIMBXXX
	61	08.09.2016	45°09.997'	153°45.419'	-	-	5,741	GKG	5	MIMBXXX
	65	09.09.2016	45°10.226'	153°44.178'	45°10.160'	153°44.052'	5,734-5,752	EBS	1	MIMBXXX
	86	15.09.2016	45°01.202'	151°06.008'	45°01.371'	151°06.001'	5,572-5,530	AGT	19	MIMBXXX
	87	16.09.2016	45°01.383'	151°05.527'	45°01.651'	151°05.522'	5,496-5,478	EBS	1	MIMBXXX

1

Table 2(on next page)

Axinulus krylovae sp. nov.

Shell measurements (mm), indices and summary statistics of indices. *L*, shell length; *H*, height; *A*, anterior end length; *W*, width.

Depository	*L*	*H*	*A*	*W*	*H/L*	*A/L*	*W/L*
Paratype IORAS XXXXX	5.1	5.5	2.3	3.5	1.078	0.451	0.686
Paratype IORAS XXXXX	5.0	5.4	1.9	3.2	1.080	0.380	0.640
Holotype IORAS XXXXX	4.9	5.3	2.0	3.4	1.082	0.408	0.694
IORAS XXXXX	4.8	5.5	2.2	3.3	1.146	0.458	0.688
IORAS XXXXX	4.8	5.2	1.8	3.1	1.083	0.375	0.646
IORAS XXXXX	4.7	4.8	2.1	3.0	1.021	0.447	0.638
Paratype MIMB XXXXX	4.7	5.3	1.8	3.6	1.128	0.383	0.766
IORAS XXXXX	4.6	4.6	1.7	2.9	1.000	0.370	0.630
Paratype IORAS XXXXX	4.5	5.1	1.9	3.2	1.133	0.422	0.711
Paratype IORAS XXXXX	4.5	4.8	1.7	3.1	1.067	0.378	0.689
IORAS XXXXX	4.3	4.5	1.9	3.1	1.047	0.442	0.721
Paratype MIMB XXXXX	4.2	4.7	1.9	3.0	1.119	0.452	0.714
Paratype SMF XXXXX	4.1	4.3	1.6	2.8	1.049	0.390	0.683
IORAS XXXXX	4.2	5.0	1.8	3.0	1.190	0.429	0.714
IORAS XXXXX	4.2	4.4	1.5	3.0	1.048	0.357	0.714
IORAS XXXXX	4.2	4.6	2.0	2.9	1.095	0.476	0.690
IORAS XXXXX	4.1	4.4	1.6	2.8	1.073	0.390	0.683
IORAS XXXXX	4.0	4.1	1.6	2.4	1.025	0.400	0.600
IORAS XXXXX	3.9	4.1	1.5	2.5	1.051	0.385	0.641
IORAS XXXXX	3.8	4.3	1.7	2.6	1.132	0.447	0.684
IORAS XXXXX	3.8	4.0	1.8	2.4	1.053	0.474	0.632
IORAS XXXXX	3.7	3.8	1.3	2.4	1.027	0.351	0.649
IORAS XXXXX	3.7	3.9	1.5	2.4	1.054	0.405	0.649
IORAS XXXXX	3.6	4.1	1.6	2.4	1.139	0.444	0.667
IORAS XXXXX	3.6	3.8	1.4	2.4	1.056	0.389	0.667
IORAS XXXXX	3.5	3.7	1.5	2.3	1.057	0.429	0.657

IORAS XXXXX	3.5	3.5	1.5	2.2	1.000	0.429	0.629
IORAS XXXXX	3.5	3.8	1.4	2.3	1.086	0.400	0.657
IORAS XXXXX	3.4	3.7	1.4	2.1	1.088	0.412	0.618
IORAS XXXXX	3.3	3.7	1.6	2.2	1.121	0.485	0.667
IORAS XXXXX	3.3	3.7	1.5	2.2	1.121	0.455	0.667
IORAS XXXXX	2.4	2.9	0.9	1.6	1.208	0.375	0.667
Statistics	*L*	*H*	*A*	*W*	*H/L*	*A/L*	*W/L*
Mean	-	-	-	-	1.083	0.415	0.671
SE	-	-	-	-	0.039	0.032	0.028
SD	-	-	-	-	0.050	0.037	0.035
Min	-	-	-	-	1.000	0.351	0.600
Max	-	-	-	-	1.208	0.485	0.766

1

Table 3(on next page)

Main differentiating characters of *Axinulus* species.

L, shell length; *H*, shell height.

Species	Maximum shell length and height (mm)	Shell	Sculpture	Escutcheon	Auricle	Lunule	Ligament	Lateral pouch	Prodissoconch length (µm) and sculpture	References
Axinulus krylovae sp. nov.	*L*=5.2 *H*=5.7	Elongated ovate to rhomboidal; anterodorsal and posterodorsal shell margins convex	Closely spaced, commarginal riblets with conspicuous radial ribs and rays and weak, irregular, undulations	Absent	Absent	Weakly defined, as a crest, raised, long, wide	Slightly visible externally as a narrow strip between valves	Large, no marked lobes	131-158; initial part with tubercle and depression, sculptured numerous, short folds and radial, long folds	Present study
Axinulus alatus sp. nov.	*L*=2.7 *H*=3.1	Oval to ovate-polygonal; anterodorsal and posterodorsal shell margins convex	Closely spaced, commarginal riblets; micro-sculpture of densely spaced pits	Weakly defined, long, narrow	Present, distinct	Weakly defined, as a weak crest, short, narrow, lanceolate	Not visible externally	Small, no marked lobes	161-174; initial part with densely spaced, short folds and wrinkles and 2 series of commarginal, long folds	Present study
Axinulus cristatus sp. nov.	*L*=3.6 *H*=3.8	Pyriform; anterodorsal and posterodorsal shell margins convex	Closely spaced, commarginal ribs and narrow, closely spaced, radial rays formed by closely spaced, finest, short,	Absent	Absent	Weakly defined, with a weak crest, long, wide	Not visible externally	No data	127; with 24 thin, almost straight folds extending from a long, high crest, located in mid-line of prodissoconch	Present study

			concentric wrinkles							
Axinulus roseus	*L*=8.7 *H*=9.3	Rhomboidal; anterodorsal shell margin concave; posterodorsal shell margin convex or straight	Conspicuous, commarginal, narrow ridges with sparse, thin, radial rays from microscopic concentric wrinkles and weak, irregular undulations; microsculpture of densely spaced pits	Well defined, very long, narrow	Absent	Well defined, sunken, long, wide	Visible externally	Large, extensively lobed	212-215; with an oblique, shallow, wide, elongated sulcus in anterior part	*Kamenev, 2020*
Axinulus oliveri	*L*=5.7 *H*=6.2	Ovate-rhomboidal; anterodorsal shell margin convex or straight; posterodorsal shell margin convex	Thin, commarginal ribs and weak, irregular undulations; microsculpture of densely spaced pits	Well defined, very long, narrow	Present, distinct	Weakly defined, with a weak crest, long, wide	Not visible externally	Large, extensively lobed	191-220; initial part with 9–12 thin, lamellated folds extending from short, plicate ridge, located in mid-line of prodissoconch	*Kamenev, 2020*
Axinulus antarcticus	*H*=2.9	Subquadrate; anterodorsal shell margin horizontal, straight; posterodorsal shell margin	Thin, commarginal ribs	Weakly defined, long, narrow	Present, distinct	Weakly defined, short, wide	Visible externally	Small, no marked lobes	115; sculptured with numerous folds, radiating from a central axis	*Zelaya, 2010*

		straight								
Axinulus philippinensis	*L*=3.2	Oblique, angular; anterodorsal shell margin convex or straight; posterodorsal shell margin convex or straight	Fine, growth lines and marginal, radial lines	Absent	Absent	No data	No data	Markedly lobed at margins	No data	*Allen, 2015*
Axinulus alleni	*L*=2.5	Subquadrate; anterodorsal shell margin straight or convex; posterodorsal shell margin convex	Very fine, growth lines	Well defined, long, narrow	Present, distinct	No data	Visible externally	Large, swollen, without lobes	No data	*Carrozza, 1981; Payne & Allen, 1991*
Axinulus brevis	*L*=2.70 *H*=3.19	Upright oval outline; sometimes pyriform; anterodorsal and posterodorsal shell margin convex	Very fine, growth lines and thin, radial riblets	Weakly defined, no sunken	Absent	Weakly defined	Visible externally	Large, elongate, no marked lobes	135-175	*Verrill & Bush, 1898; Payne & Allen, 1991*
Axinulus croulensis	*L*=1.8 *H*=2.0	Upright oval or almost circular outline; anterodorsal	Very fine, commarginal lines and growth stops,	Absent	Indistinct	Absent	Visible externally	Large, with small projecting lobes along dorsal	121-141	*Payne & Alen, 1991; Oliver & Killeen,*

		shell margin horizontal, straight; posterodorsal shell margin convex	mostly glossy with a radial texture					margin		*2002*
Axinulus subequatorius	*L*=3.3 *H*=3.5	Pyriform; anterodorsal and posterodorsal shell margins convex	Fine, ill-defined growth lines	Present	Absent	No data	No data	With a number of small peripheral lobes	No data	*Payne & Alen, 1991*

1

Table 4(on next page)

Additional material of *Axinulus alatus* sp. nov. examined in the present study.

OG, Okean grab (0.25 m^2); GKG, giant box corer (0.25 m^2); EBS, epibenthic sledge; ST, Sigsbee trawl; *N*, number of live specimens.

Ship, cruise no.	Station	Date	Start		End		Depth (m)	Gear	*N*	Depository
			Latitude ºN	Longitude ºE	Latitude ºN	Longitude ºE				
Abyssal slope of the Kuril Islands, Pacific Ocean										
Akademik M.A. Lavrentyev 71	9-1	27.07.2015	46°16.082'	152°02.060'	-	-	3,432	GKG	10	MIMBXXX
	9-6	26.07.2015	46°16.103'	152°02.004'	46°16.132'	152°03.036'	3,436-3,377	EBS	2	MIMBXXX
	9-7	26.07.2015	46°16.129'	152°02.440'	46°16.070'	152°03.324'	3,409-3,377	EBS	1	MIMBXXX
Commander Basin, Bering Sea										
Akademik Mstislav Keldysh 22	2309	31.07.1990	55°13.2'	167°29.07'	55°12'	167°26.7'	3,957-3,978	ST	73	IORASXX
	2316	05.08.1990	55°36.1'	167°23.04'	55°35'	167°24.5'	4,294-4,200	ST	1	IORASXX
Kodiak Island, Gulf of Alaska, Pacific Ocean										
Vityaz 45	6095	08.05.1969	57°37.7'	148°34.5' W	-	-	3,200	OG	2	MIMBXXX

1

Table 5(on next page)

Axinulus alatus sp. nov.

Shell measurements (mm), indices and summary statistics of indices. *L*, shell length; *H*, height; *W*, width; *A*, anterior end length.

Depository	*L*	*H*	*A*	*W*	*H/L*	*A/L*	*W/L*
Paratype MIMB XXXXX	2.7	2.8	1.1	1.7	1.037	0.407	0.630
Paratype IORAS XXXXX	2.6	2.9	1.0	1.7	1.115	0.385	0.654
Paratype IORAS XXXXX	2.5	2.8	1.0	1.7	1.120	0.400	0.680
Paratype IORAS XXXXX	2.6	2.8	1.0	1.6	1.077	0.385	0.615
Paratype IORAS XXXXX	2.5	2.8	1.0	1.6	1.120	0.400	0.640
Paratype IORAS XXXXX	2.5	2.6	1.0	1.5	1.040	0.400	0.600
Holotype MIMB XXXXX	2.4	2.6	1.0	1.5	1.083	0.417	0.625
Paratype SMF XXXXX	2.3	2.6	0.9	1.4	1.130	0.391	0.609
IORAS XXXXX	2.4	2.6	0.9	1.5	1.083	0.375	0.625
IORAS XXXXX	2.3	2.5	0.8	1.4	1.087	0.348	0.609
IORAS XXXXX	2.2	2.4	0.8	1.4	1.091	0.364	0.636
IORAS XXXXX	2.2	2.4	0.9	1.3	1.091	0.409	0.591
IORAS XXXXX	2.2	2.4	0.8	1.3	1.0911	0.364	0.591
IORAS XXXXX	2.1	2.3	0.7	1.3	1.095	0.333	0.619
IORAS XXXXX	2.1	2.3	0.8	1.3	1.095	0.381	0.619
IORAS XXXXX	2.1	2.5	0.7	1.2	1.190	0.333	0.571
IORAS XXXXX	2.1	2.3	0.7	1.3	1.095	0.333	0.619
IORAS XXXXX	2.0	2.4	0.7	1.4	1.200	0.350	0.700
IORAS XXXXX	2.0	2.2	0.9	1.3	1.100	0.450	0.650
IORAS XXXXX	2.0	2.3	0.7	1.3	1.150	0.350	0.650
IORAS XXXXX	2.0	2.2	0.6	1.3	1.100	0.300	0.650
IORAS XXXXX	2.0	2.1	0.8	1.2	1.050	0.400	0.600
IORAS XXXXX	1.9	2.2	0.6	1.2	1.158	0.316	0.632
IORAS XXXXX	1.9	2.0	0.7	1.2	1.053	0.368	0.632
IORAS XXXXX	1.9	2.1	0.6	1.2	1.105	0.316	0.632
IORAS XXXXX	1.9	2.1	0.8	1.1	1.105	0.421	0.579

IORAS XXXXX	1.9	2.1	0.7	1.1	1.105	0.368	0.579
IORAS XXXXX	1.9	2.1	0.8	1.1	1.105	0.421	0.579
IORAS XXXXX	1.8	2.0	0.7	1.1	1.111	0.389	0.611
IORAS XXXXX	1.7	1.9	0.5	1.0	1.118	0.294	0.588
IORAS XXXXX	1.6	1.8	0.5	0.9	1.125	0.313	0.563
IORAS XXXXX	1.5	1.7	0.5	0.9	1.133	0.333	0.600
Statistics	*L*	*H*	*A*	*W*	*H/L*	*A/L*	*W/L*
Mean	-	-	-	-	1.105	0.369	0.618
SE	-	-	-	-	0.026	0.033	0.024
SD	-	-	-	-	0.037	0.039	0.031
Min	-	-	-	-	1.037	0.294	0.563
Max	-	-	-	-	1.200	0.450	0.700

1